May 2013

Infrared Light Induced Bending of Liquid Crystalline Elastomer Composite-Silicone Bilayer Films

Maika Moua
University of Wisconsin-Milwaukee

INFRARED LIGHT INDUCED BENDING OF LIQUID CRYSTALLINE ELASTOMER COMPOSITE-SILICONE BILAYER FILMS

by

Maika Moua

A Thesis Submitted in

Partial Fulfillment of the

Requirements for the Degree of

Master of Science

in Chemistry

at

The University of Wisconsin-Milwaukee

May 2013

ABSTRACT

INFRARED LIGHT INDUCED BENDING OF LIQUID CRYSTALLINE ELASTOMER COMPOSITE-SILICONE BILAYER FILMS

by

Maika Moua

The University of Wisconsin-Milwaukee, 2013

Under the Supervision of Professor Carolyn Aita

This research centers on infrared (IR) light-induced bending of liquid crystalline elastomers (LCE) composite-silicone bilayer films. Two new developments are presented in this thesis. First, the reversible infrared (IR) induced bending of 0.1% (w/w) single walled nanotube (SWNT)-LCE/silicone bilayer films were successfully prepared and used for fabrication of functioning devices such as folding, grabbing, and crawling structures. Second, the use of adding a filler (absorbs specific wavelength range), such as Dye 1002, into the LCE matrix achieved wavelength selectivity in LCE systems. The 0.2% (wt/wt) Dye 1002-LCE/silicone bilayer films demonstrated bending under a 980 nm laser source but no bending under a 1342 nm laser source. These developments are evidence that LCE systems can be used for making a variety of IR light-induced functional devices and that LCE systems can be tuned to absorb a specific wavelength range of IR light by adding a filler such as Dye 1002 into the LCE network.

TABLE OF CONTENTS

LIST OF FIGURES

LIST OF TABLES

ACKNOWLEDGEMENTS

I would like to thank:

1) my major professor, Dr. Carolyn Aita, for accepting me into her professional academic family, guidance in writing my thesis, motivational support and encouragement.

2) my committee members: Dr. Carolyn Aita, Dr. Joseph Aldstadt, and Dr. Kristene Sererus for their guidance in revising this thesis, knowledgeable criticism and encouragement.

3) Dr. Peter Geissinger and Dr. Joseph Aldstadt for their support and guidance in completing this program.

4) my husband and family, for always believing in me and providing me with unconditional love and support.

5) Dr. Jian Chen for supervising the project.

6) Ryan Kohlymeyer for his support and companionship.

This study was supported by NSF grant #0856162.

I. Introduction

A. Background

Smart materials are of growing interest because of their ability to perform specific functions as they respond to environmental changes. In liquid crystalline elastomers (LCEs), autonomous deformation is caused by thermal changes in the system that can be stimulated by an external source, such as heat,[1-4] light,[5-15] pH,[16] or electric field.[17] LCEs have two phases which enable them to undergo reversible shape change, mimicking the physical motion of a muscle contraction: the nematic phase and the isotropic phase. During the nematic phase, the mesogen (monomer) units are aligned along the backbone of the polymer chain. When heated above the nematic-isotropic transition temperature (T_{NI}), the material exhibits the isotropic phase, in which the mesogen units become disordered. Consequently, the material contracts. After the heat source is turned off and the temperature of the material falls below the T_{NI}, the mesogen units will re-align themselves along the polymer backbone. This procedure allows the LCE material to elongate. Response to temperature changes permit reversible contraction and elongation in LCE systems. Hence, grabbing, folding, and crawling structures can be fabricated.

One major disadvantage of a pure nematic LCE system is its poor thermal conductivity. However, it has been found that the addition of a thermally conductive material to an LCE system can increase the response time.[18] In earlier work done by Yang et al., single-walled carbon nanotubes (SWNTs) were used as fillers mixed into the LCE network.[19] Since SWNTs have excellent thermal conductivity and show strong

absorptions in the infrared (IR) regions, this allows for thermal heating of the LCE material by an infrared light source. By adding poly(*p*-phenyleneethynylene) (PPE)-solubilized SWNTs into the LCE film, IR actuation was achieved.

Extending Yang and coworkers' work are two hypotheses that will be discussed. The first hypothesis is that the above mentioned contraction can be utilized to achieve a bending motion. The exploration of IR light-induced reversible shape deformation of LCE systems is important for ultimate fabrication of a fully-functioning device. To achieve a remotely controlled autonomous motion in non-biological systems is intriguing, but to turn that slight motion into a larger execution is even more fascinating.

The second is that a specific absorbance range (wavelength selectivity range) will be used to investigate the thermal effect of introducing a filler into the LCE system. By tuning the filler, wavelength selectivity in LCE systems can hopefully be achieved.

B. Current developments

Researchers have already shown that LCEs containing azobenzene moieties can reversibly bend under ultraviolet (UV) light and unbend under visible light.[8,20] Azobenzene is most stable in the *trans*-conformation. Absorption of UV light causes azobenzene molecules to switch from *trans* to *cis* conformation and allows for contraction of LCE material. Absorption of visible light switches the molecule conformation from *cis* to *trans* and allows for elongation. *Cis-trans* isomerization of a simple azobenzene structure is shown in Figure 1.

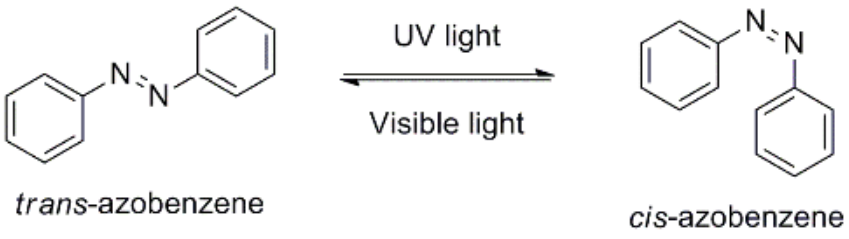

Figure 1. Isomerization of azobenzene.

Using azobenzene moieties, current state of the art studies from Ikeda's[8] group found that polarized UV light can be used to control the direction of bending in a polymer film. In addition, they found that shape deformation induced by UV and visible light can be used to make functional devices.[20] This class of LCEs, however, is limited to only UV and visible light.

In LCE systems without *cis-trans* isomerization of azobenzene moieties, fillers with specific wavelength absorbance can be used to induce a photomechanical response in the visible spectrum. In a study done by Palffy-Muhoray's group,[21] LCE films containing a methylsiloxane backbone and biphenyl sidechains were made with an azobenzene dye. This azobenzene dye absorbs radiation in the visible spectrum, which allows the LCE film to be activated by visible light. The absorption of visible light is converted to thermal energy and causes the film to contract as though it were heated above its T_{NI}. These investigators were able to engineer a film with swimming capabilities as it responds to visible light.[21]

In non-LCE systems, there have been reports of bilayer films with the ability to fold in response to light.[22-23] These soft material robotics have the ability to crawl and to pick up and release objects in response to pressure.[24-25]

The research conducted here differs from the aformentioned studies and extends the state of the art because it shows that independently functioning devices can be created from LCE material by IR-induction instead of UV or visible light. To accomplish this goal, the LCE system that was chosen for this study is one that does not contain active azobenzene moeities. Mixing fillers with absorption in the IR region into the LCE material will allow for IR induced response. The IR light-induced reversible contraction and elongation of LCE films is then converted to a reversible bending motion. Using this reversible bending motion, different devices are designed to serve a functional purpose. *As a result of this new development, photomechanical response of LCE materials are not limited to UV or visible light.*

The second part of this study focuses on the absorbance of a specific wavelength of light in LCE films which can be controlled by using different fillers. It has been noted that LCE can convert light to thermal energy by absorption of light. By using fillers with a unique absorption spectrum in LCE films, only light with wavelength within that specific range can be used to induce LCE response. This wavelength selective feature adds another very important property to LCE films.

II. Preparation and Characterizations of LCE/Silicone Bilayer Hinges

A. Materials

We used the following compounds for preparation of the LCE films. Figure 2 shows the four components that make up the LCE films.

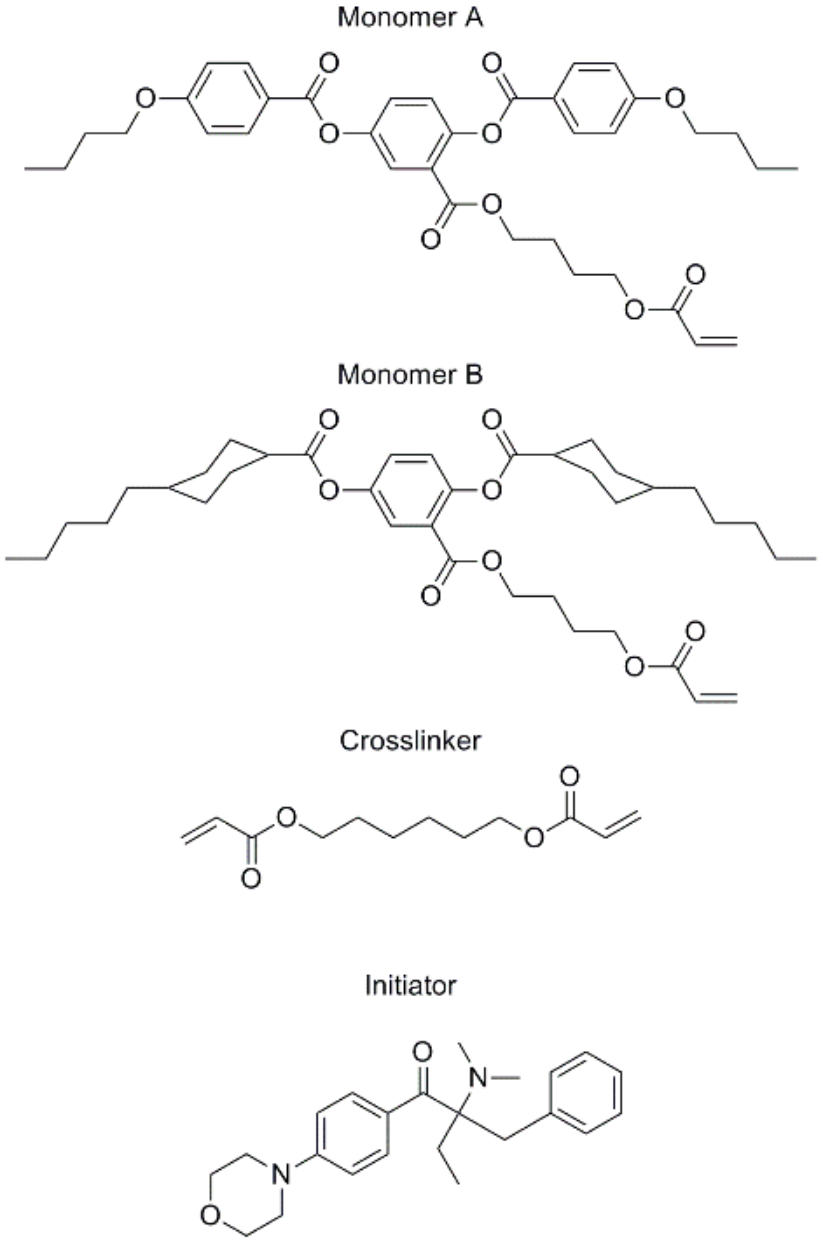

Figure 2. Components of LCE film.[26]

The following chemicals were used for synthesizing monomers A and B: 2,5-dihydroxybenzoic acid, benzyl bromide, and N,N'-dicyclohexylcarbodiimide (DCC) (Alfa Aesar). 4-Pyrrolidinopyrdine and 4-pentylcyclohexylcarboxylic acid (TCI America). 4-Butoxybenzoic acid and chloroform (Sigma-Aldrich). Compressed hydrogen, nitrogen 5.0 Grade UHP, and Argon 5.0 Grade UHP (Praxair).

The crosslinker (1,6-hexanediol diacrylate) and the initiator (Irgacure 369) was used as received: 1,6-hexanediol diacrylate (Alfa Aesar), Irgacure 369 (Sigma Aldrich).

(4"-Acryloyloxybutyl) 2,5-di(4'-butyloxybenzoyloxy) benzoate (monomer A) and (4"-acryloyloxybutyl) 2,5-di(4'-pentylcyclohexylcarboxyloxy) benzoate (monomer B) were synthesized, purified, and characterized by proton-nuclear magnetic resonance (^{1}H-NMR) based upon a procedure described by Thomsen et al.[26] The schemes for synthesizing monomer A and monomer B are shown in Figure 3 and Figure 4, respectively.

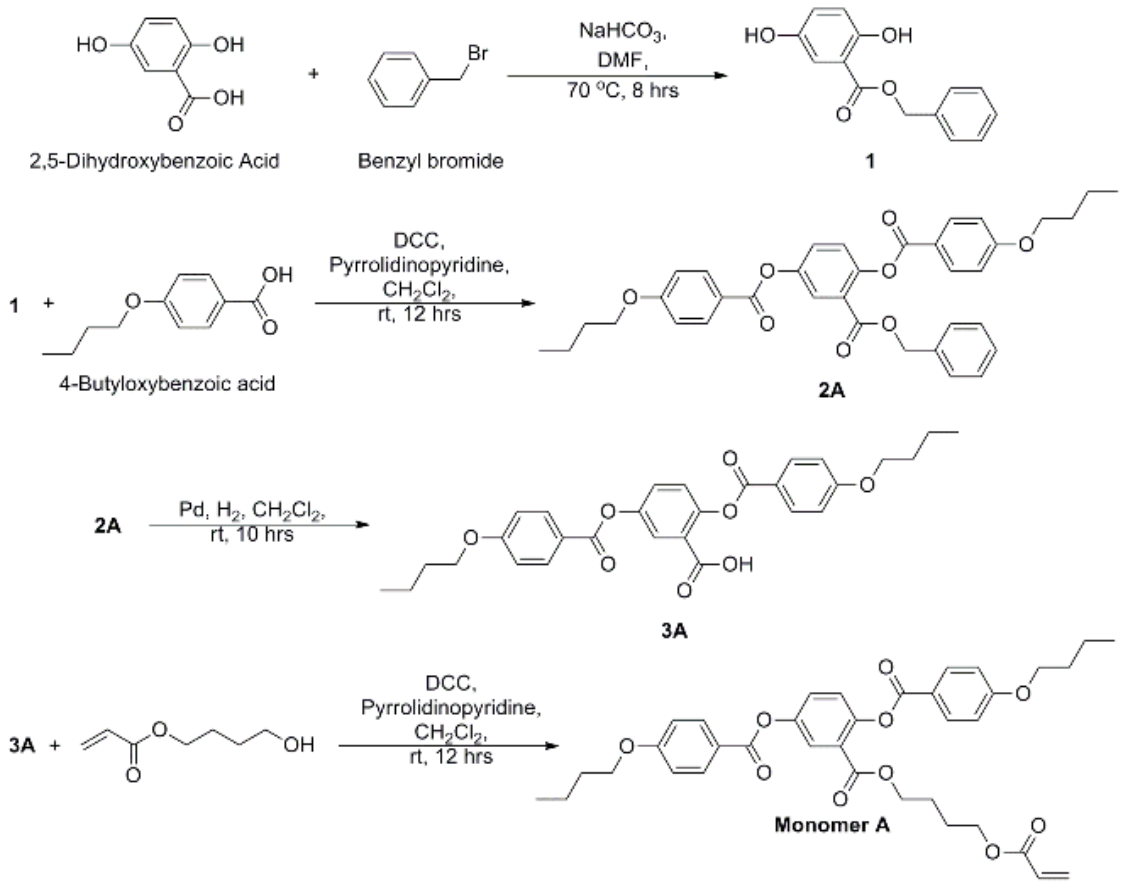

Figure 3. Synthesis scheme for monomer A.[26]

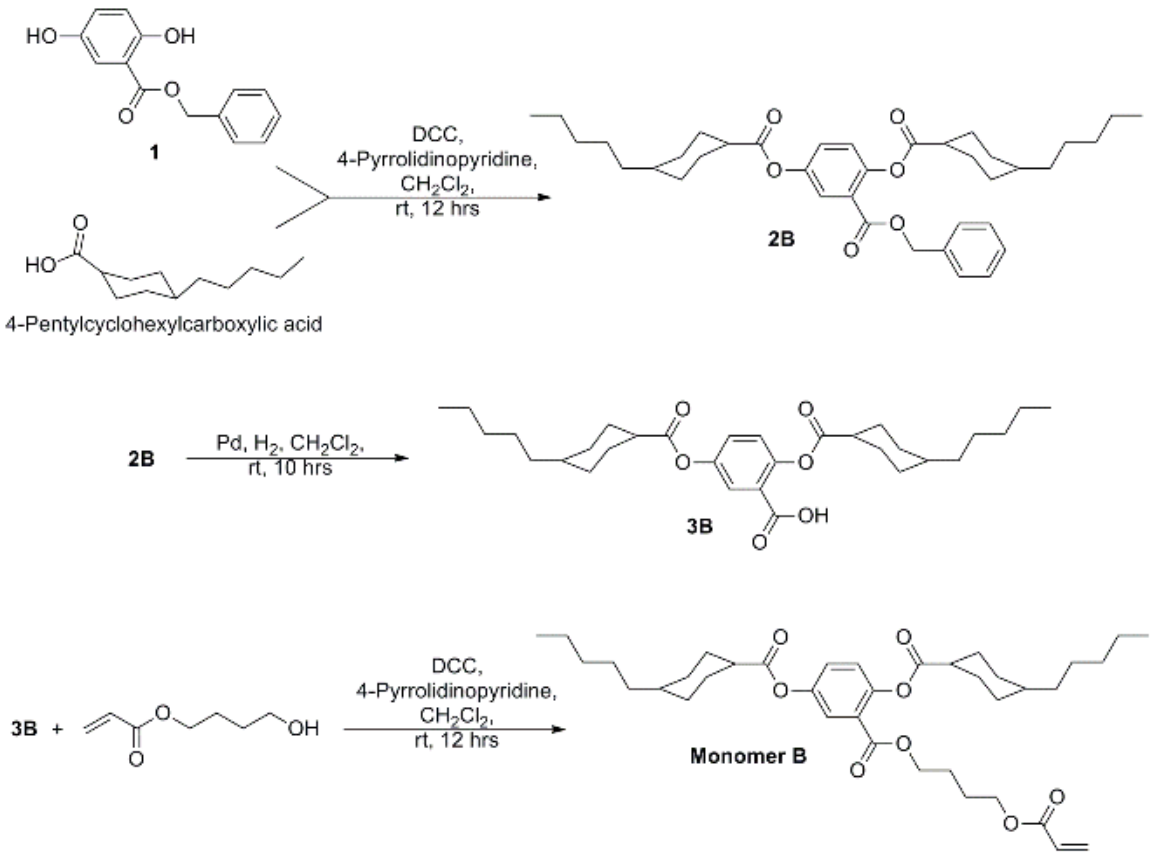

Figure 4. Synthesis scheme for monomer B.[26]

^{1}H-NMR spectra of monomer A and monomer B were collected in $CDCl_3$ using a Bruker Spectrospin 300 MHz or Bruker 500 MHz instrument. The ^{1}H-NMR spectra obtained of monomer A and monomer B is shown in Figure 5 and Figure 6, respectively. (Monomer A: ^{1}H- NMR ($CDCl_3$) δ (ppm): 1.0 (t, 6H, -CH_3), 1.5-1.7 (m, 8H, -CH_2-), 1.8-1.9 (m, 4H, -CH_2-), 4.0-4.1 (m, 6H, -OCH_2), 4.2 (t, 2H, OCO-CH_2), 5.8 (m, 1H, CH_2=C), 6.1 (m, 1H, C=CH-), 6.4 (m, 1H, CH_2=C), 7.0-7.2 (m, 4H, ArH), 7.3-7.5 (m, 2H, ArH), 7.9 (s, 1H, ArH), 8.2-8.3 (m, 4H, ArH).) (Monomer B: ^{1}H- NMR ($CDCl_3$) δ (ppm): 0.88-0.90 (m, 6H, -CH_3), 0.9-1.0 (m, 4H, -CH (EQ)), 1.2-1.3 (m, 18H, -CH

(AX)), -CH_2-), 1.5-1.6 (m, 4H, -CH_2-), 1.8-1.9 (m, 8H, -CH (AX, EQ)), 2.1-2.2 (m, 4H, -CH (AX)), 2.4-2.6 (m, 2H, -CH (AX)), 4.2 (t, 2H, -CH_2-OCO), 4.3 (t, 2H, $OCOCH_2$), 5.8 (m, 1H, CH_2=C), 6.1 (m, 1H, C=CH-), 6.4 (m, 1H, CH_2=C), 7.1 (m, 1H, ArH), 7.3 (m, 1H, ArH), 7.7 (s, 1H, ArH).)

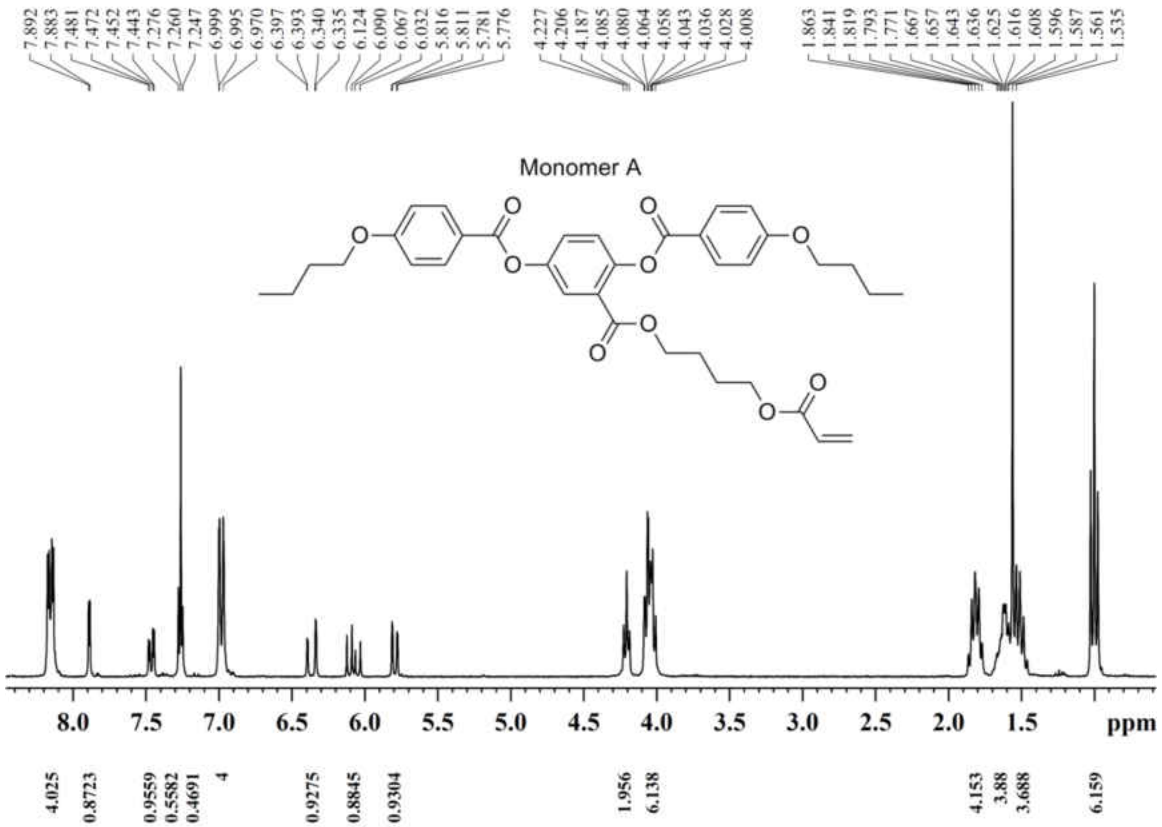

Figure 5. ^{1}H-NMR of Monomer A.

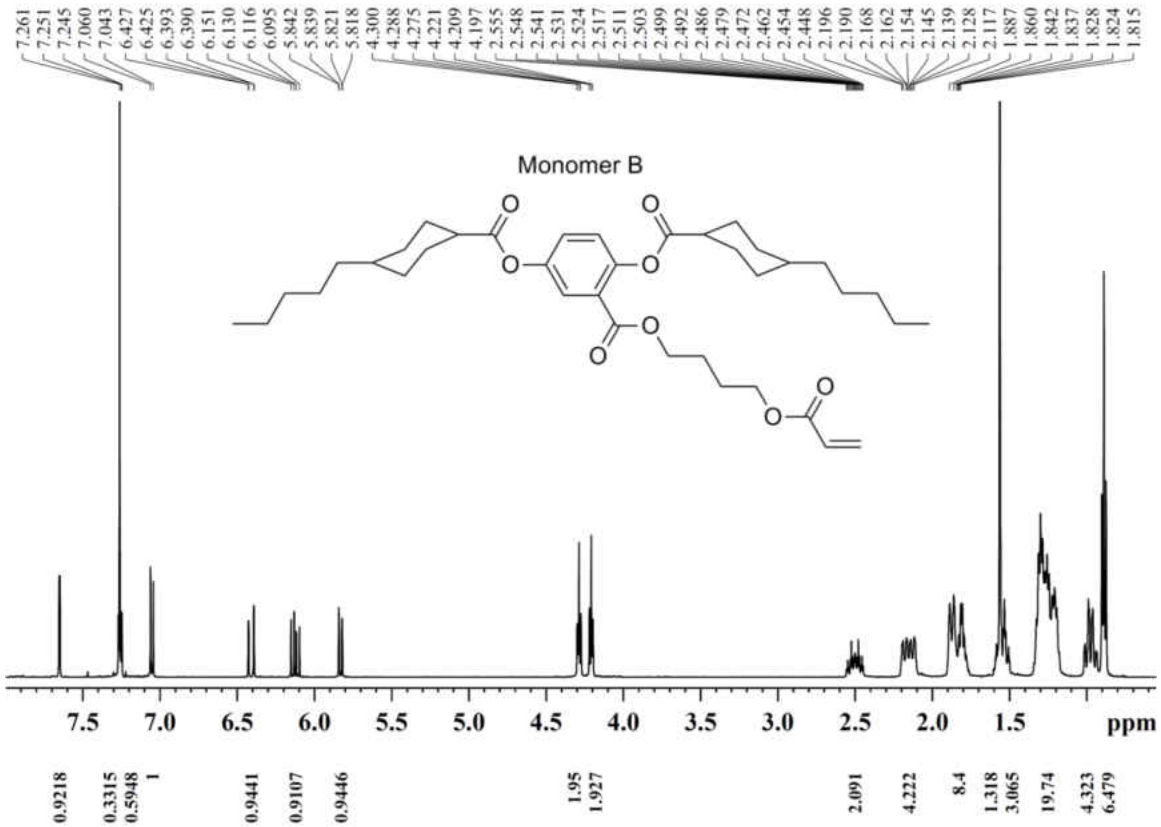

Figure 6. ^{1}H-NMR of Monomer B.

.

The following materials were used as fillers to mix into the LCE films: Purified HiPco-SWNTs (Lot#: P0353) were purchased from Carbon Nanotechnologies, Inc. Dye 1002 was purchased from QCR Solutions.

The following materials were used for making functional structures: Ecoflex 00-30 (Part 1A and Part 1B) was purchased from Smooth-On, Inc. Poly(bisphenol A carbonate) (PC) was purchased from Sigma Aldrich. 3145 RTV Silicone Adhesive was purchased from Dow Corning.

B. Preparation and Characterizations of 0.1 wt% SWNT-LCE Films

A 0.25 mg/mL solution of PPE–SWNTs (PPE:SWNT 1:2 by weight) in chloroform was prepared according to literature.[26] The SWNT loading-level in the film was based only on purified SWNT material and excluded the PPE material. Monomer A (45.5 mg, 0.072 mmol), monomer B (69.1 mg, 0.108 mmol), 1.6-hexanediol (3.3 mg, 0.0146 mmol) and Irgacure 369 (0.33 mg, 0.00090 mmol) were transferred into a vial and mixed together. Next, 0.46 mL of 0.25 mg/mL PPE-SWNT solution in chloroform was added. After most of the chloroform evaporated, the thick solution was casted onto a 3 cm^2 rectangular area of a PTFE dish and allowed to turn into a paste.

The paste was heated on a hot plate at 90 °C to remove solvent and air bubbles. The mixture was vacuum-dried at 40 °C for 10 min, followed by 10 min of N_2 purging at 40 °C. A Blak-Ray Long Wave (365 nm) Ultraviolet Lamp Model B 100AP was used for photopolymerization. The UV radiation power was measured using a Newport power meter model 1918-C with a UV detector (918D-UV-OD3). The top side of the film was first partially photopolymerized at 40 °C under N_2 with 8 min of 1.24 mW/cm^2 UV-light exposure. The film was peeled from the PTFE dish and flipped upside down. The bottom side of the film was vacuum-dried at 40 °C for 10 min, followed by 10 min of N_2 purging at 40 °C. The bottom side of the film was then partially photopolymerized at 40 °C under N_2 with 8 min of 1.24 mW/cm^2 UV-light exposure.

The partially cured film was clamped on both ends with clips and placed in an oven. The film was stretched to 275-300% in the oven at ~40 °C by hanging 50 g of weight onto the bottom clips. After stretching, the film was left overnight at room

temperature while under tension. Weights (50g) were left on the bottom clip to prevent the film from shrinking overnight. Weights (50g) were replaced by 20 g weights during final curing to prevent the film from breaking. Final curing was done by subjecting each side of the film to 10 min of 26.8 mW/cm^2 UV-light exposure. After final curing, the film was annealed at 40 °C for 2 h. Stretching ratio of the annealed films range from 180% to 190%. The stretching ratio in Equation 1 is defined below, where L_o is the initial length of the film and L is the final length of the film. Equation 2 defines the stretching ratio reported in a previous work.[19] 180% stretching ratio reported here is equivalent to 80% stretching ratio from the previous work.

$$\textit{Stretching Ratio} = (L/L_o)(100\%) \quad (1)$$

$$\textit{Stretching Ratio} = ((L-L_o)/L_o)(100\%) \quad (2)$$

The film was characterized as follows:

Film thickness was measured using a Mitutoyo Digital Micrometer. The typical thickness of a 0.1 wt% SWNT-LCE film was 249 +/- 9 μm.

Differential scanning calorimetry (DSC) thermograms were acquired using a TA Instruments DSC Q10 under Ar. The sample was first heated from 0 °C to 120 °C at a rate of 10 °C/min inside the DSC instrument. The sample was then removed from the DSC instrument and was quenched by submerging into liquid N_2. The sample was placed back in the DSC instrument and the spectrum (Figure 7) was collected as the sample was heated from -60 °C to 100 °C at a rate of 10 °C/min. The nematic-isotropic temperature of a representative 0.1 wt% SWNT-LCE film was 65 °C, as determined from the DSC measurement. The DSC thermogram of a 0.1 wt% SWNT-LCE film is shown

in Figure 7. The T_{NI} that was reported in a previous work[19] was 52.5 °C. However, the T_{NI} results that were provided through personal communication were found to be 60 °C. The difference in this nematic-isotropic temperature compared to previous work[19] is possibly due to a longer final curing time and additional thermal treatment (annealing) of the film in order to equilibrate it. Reference 19 does not report an annealing step.

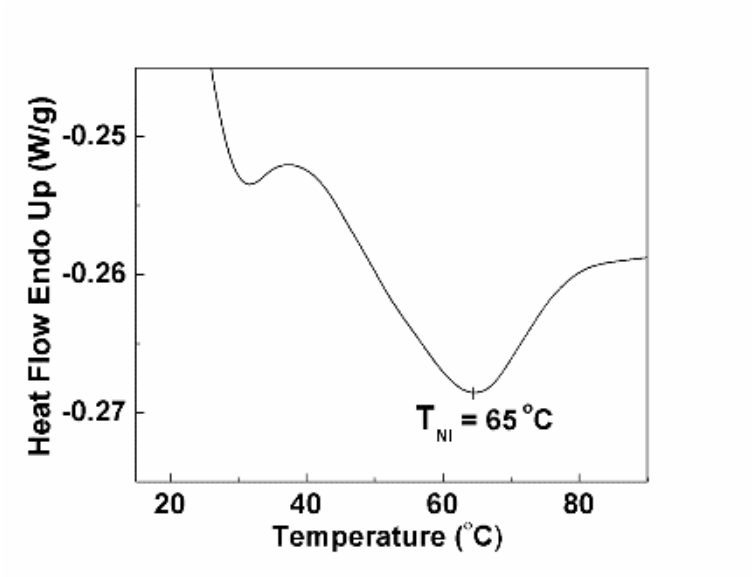

Figure 7. DSC thermogram of 0.1 wt% SWNT-LCE film.

C. Preparation and Characterizations of 0.2 wt% Dye 1002-LCE Films

Monomer A (45.5 mg, 0.072 mmol), monomer B (69.1 mg, 0.108 mmol), 1.6-hexanediol (3.3 mg, 0.0146 mmol) and Irgacure 369 (0.33 mg, 0.00090 mmol) were transferred into a vial and mixed together. Next, 0.12 mL of 1 mg/mL Dye 1002 solution in chloroform was added. After most of the chloroform evaporated, the thick solution was casted onto a 3 cm^2 rectangular area of a PTFE dish and allowed to turn into a paste.

The paste was heated on a hot plate at 90 °C to remove solvent and air bubbles. The mixture was vacuum-dried at 40 °C for 10 min, followed by 10 min of N_2 purging at 40 °C. The top side of the film was first partially photopolymerized at 40 °C under N_2 with 7 min of 1.24 mW/cm^2 UV-light exposure. The film was peeled from the PTFE dish and flipped upside down. The bottom side of the film was vacuum-dried at 40 °C for 10 min, followed by 10 min of N_2 purging at 40 °C. The bottom side of the film was then partially photopolymerized at 40 °C under N_2 with 9 min of 1.24 mW/cm^2 UV-light exposure.

The partially cured film was clamped on both ends with clips and placed in an oven. The film was stretched to 300% in the oven at ~40 °C by hanging 50 g of weight onto the bottom clips. The film was left overnight at room temperature while under tension. Final curing was done by subjecting each side of the film to 10 min of 26.8 mW/cm^2 UV-light exposure. After final curing, the film was annealed at 40 °C for 2 h. Stretching ratio of the annealed films range from 178% to 186%.

Typical 0.2 wt% Dye 1002 films were 245 +/- 11 μm thick. The nematic-isotropic temperature (determined from the DSC measurement) of a representative 0.2 wt% Dye 1002-LCE film was 64 °C as shown in Figure 8.

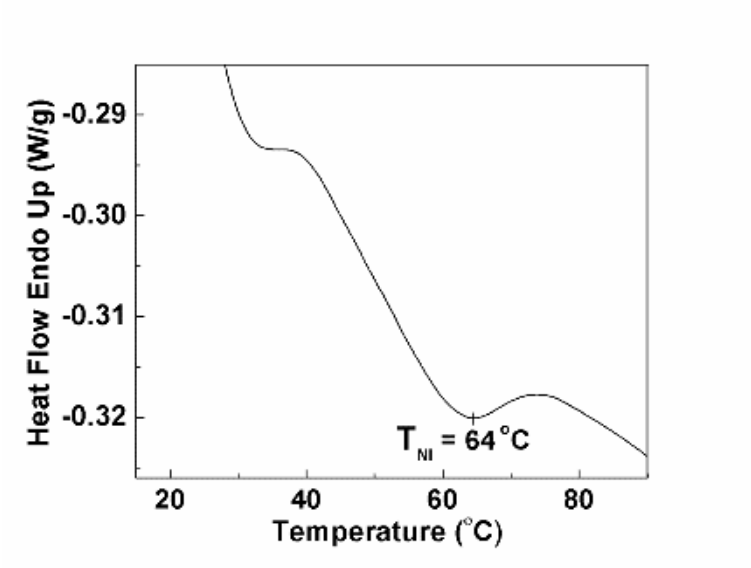

Figure 8. DSC thermogram of 0.2 wt% Dye 1002-LCE film.

D. Characterization of LCE films by Attenuated Total Reflectance - Infrared Spectroscopy (ATR-IR)

Characterization of LCE films was also done by using attenuated total reflectance - infrared spectroscopy (ATR-IR) using a Thermo Nicolet Nexus 670 FT-IR Thermo Fisher Smart OMNI-Sampler accessory. The OMNI-Sampler is equipped with a germanium crystal and a metal tower.

During the UV curing step of the LCE film preparation, polymerization is expected to occur. There are a few aspects that can determine whether polymerization has taken place or not. First, once polymerized, the film should look rubbery and somewhat glassy. It should also be able to stretch when a force is applied at 40 °C. A film that is not polymerized, mainly a paste, will break when a force is applied.

Transparency of the LCE film can also determine if polymerization has occurred. Although these features can help us determine whether or not polymerization has occurred, it is still important to provide spectral evidence supporting this process.

ATR-IR was used to determine whether polymerization took place during the UV curing step. ATR-IR spectra were obtained from a Nicolet iS10 FT-IR Spectrometer, equipped with Smart OMNI-Sampler. The Smart OMNI-Sampler is made with germanium crystal.

Figure 9 shows ATR-IR spectra of a 0.1 wt% SWNT-LCE paste (before polymerization) and 0.1 wt% SWNT-LCE film (after polymerization). To make the paste, the initiator (0.33 mg, 0.00090 mmol) and crosslinker (3.3 mg, 0.0146 mmol) were mixed into monomer A (45.5 mg, 0.072 mmol) and monomer B (69.1 mg, 0.108 mmol). A chloroform solution of PPE-SWNT was then added to this mixture. The contents were mixed thoroughly until all of the chloroform evaporated. A small amount (roughly 5-10 mg of this mixed paste) was then used for ATR-IR analysis.

For ATR-IR analysis of the polymerized film sample, a small sample (roughly 2 mm by 2 mm) of the 0.1 wt% SWNT-LCE film was used. This film sample was obtained after the thermal annealing step, which is the final step of the LCE film preparation (the step right before attaching the LCE film to a silicone film).

To collect the ATR-IR spectra, each sample was placed on the germanium crystal plate. The tower was adjusted by rotating the knob until it clicks once. The knob was located on the top of the tower. This allowed the tower to move downwards onto the

sample. The click served as an indication that maximum pressure was applied to the sample. The spectra were collected at a resolution of 4 with 128 scans.

In Figure 9, there are three peaks that will be discussed when comparing the spectrum of the paste to the film. The paste consists of both monomers and crosslinker, which contain acryloyl groups (H_2C=CH–C(=O)–). Once polymerization occurs, the vinyl groups (H_2C=CH–) are no longer present. The C=C (of the vinyl group) twisting vibration (812 cm^{-1}) and stretching vibration (1636 cm^{-1}) are present in the spectrum of the LCE paste but not observed in the spectrum of the LCE film. The C=O stretching vibration (1710 cm^{-1}) of the terminal acryloyl group is also not observed in the spectrum of the film. We speculate that the C=O stretching vibration (1710 cm^{-1}) from the terminal acryloly group is different from other C=O stretching vibrations (1730 cm^{-1}) in the monomers. However, once the film is polymerized, although the C=O bond does not change, the stretching vibration becomes similar to other C=O stretching vibrations. Therefore a separate stretching vibration frequency appears in the spectrum of the paste but is not present in the spectrum of the film.

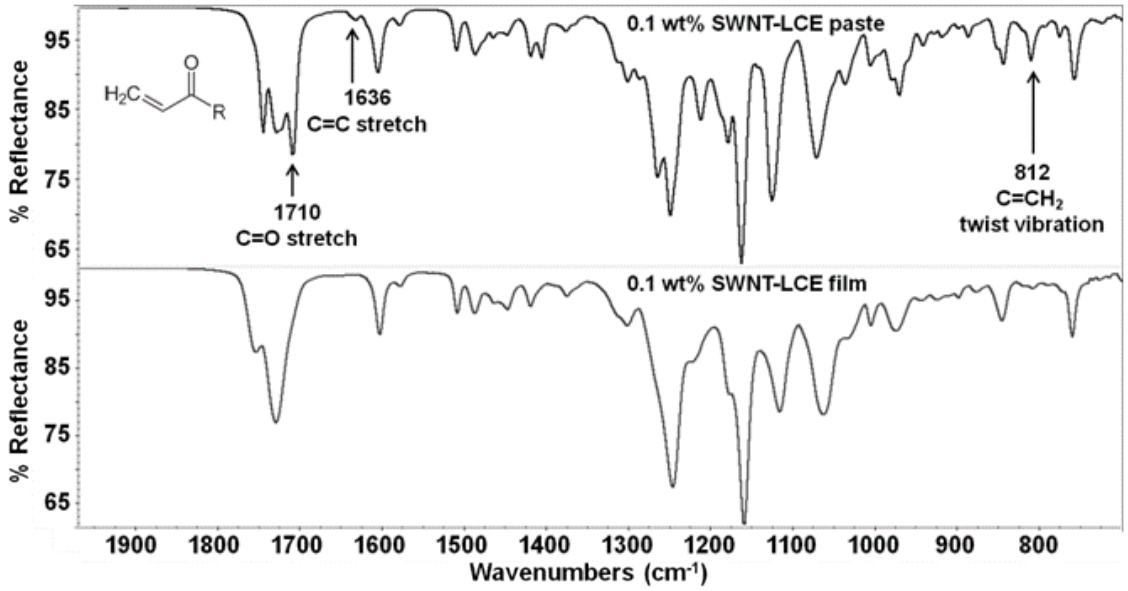

Figure 9. ATR-IR spectra of 0.1 wt% SWNT-LCE paste and film.

The ATR-IR spectra obtained for 0.2 wt% Dye 1002-LCE paste and film also revealed similar spectrum.

E. Preparation and Characterization of Silicone Films and PC Films

Silicone films with a thickness of ~150 μm, ~350 μm or ~650 μm were prepared. To make 150 μm thick silicone films, 0.4 mL of Ecoflex 00-30 Part 1A was added to 0.4 mL of Ecoflex 00-30 Part 1B. A minimal amount (1-2 mL) of chloroform was added to the mixture to provide a thin free-flowing liquid. The mixture was casted onto a 8 cm diameter PTFE dish. The chloroform was evaporated at 40 °C followed by curing of the film at 80 °C overnight. To make 350 μm thick silicone films, 0.80 mL of Part 1A and 0.80 mL of Part 1B were mixed together. To make 650 μm thick silicone films, 1.6 mL

of Part 1A was mixed with 1.6 mL of Part 1B. Curing temperature and time was the same.

PC films (100 μm) were prepared. PC solution in chloroform (3 mL of 100 mg/mL) was poured into a 6 cm diameter PTFE dish. The dish was covered with a larger glass dish to allow for slow evaporation.

F. Preparation of 0.1 wt% SWNT-LCE/Silicone Bilayer Hinges

F. 1. Preparation of SWNT-LCE/Silicone Bilayer Hinges for Bending Experiments

For curvature studies, 0.1 wt% SWNT-LCE/silicone bilayer films (14 cm and 23 cm long) were prepared. A diagram of a bilayer film is shown in Figure 10 where *L* is the length of the bilayer film, *w* is the width of the bilayer film, t_1 is the thickness of the LCE film and t_2 is the thickness of the silicone film. Exact dimensions of the films can be found in the results section.

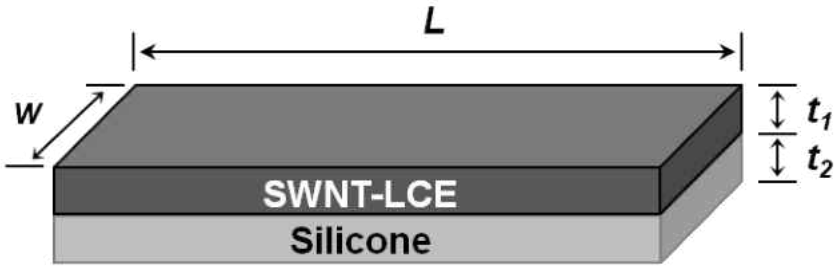

Figure 10. Diagram of 0.1 wt% SWNT-LCE/silicone bilayer hinge.

To make bilayer films, a thin layer of silicone adhesive was applied to 0.1 wt% SWNT-LCE films of desired length and width. A razor was used to remove the excess adhesive. The 0.1 wt% SWNT-LCE films were gently placed onto previously prepared silicone films of desired thicknesses. The silicone adhesive was allowed to cure for 4 h at room temperature. Once the silicone adhesive dried, a razor was used to cut the silicone film, matching the silicone length and width to that of the 0.1 wt% SWNT-LCE length and width.

The 0.1 wt% SWNT-LCE/silicone bilayer films were irradiated with a 100 W Torch flashlight (white light) that was purchased from Wicked Lasers. The Torch flashlight is equipped with a 100 W halogen bulb. Since the Torch is very bright, the heat emitted from the Torch often causes the IR filters to break. The majority of the experiments in this section were done using the irradiation of the Torch without IR filters. Additional experiments were conducted to conclude that the Torch flashlight mainly emits IR light.

The power of the Torch flashlight was measured using a Newport power meter model 1918-C with an IR detector (918D-IR-OD3). Since this meter is only accurate in measuring power or intensity of a specific wavelength of light (not a range), the intensity of the Torch at varying distances could not be determined. Instead, the power meter was used to determine the percentage of IR light that comes from the Torch flashlight. The light emitted from the Torch flashlight was calculated to be 90.5% IR light. To determine this percentage, Equation 3 was used, where P_{total} is the measured power of total white light at a given distance and P_{850} is the measured power of light that passed through the 850 nm cut on filter at the same distance. This is to ensure that the light passed through

the filter is indeed IR light. The wavelength range for the near and part of the mid-IR light is from 750 nm to 2000 nm.

$$Percent\ of\ IR\ Light = (P_{850}/P_{total})(100\%) \quad (3)$$

Power measurements of total white light were taken from distances of 15 cm, 23 cm, and 30 cm. Using an 850 nm cut-on filter to cover the light source, power measurements of the source was taken again at the distances indicated above. Two different settings (1000 nm and 1064 nm) were used when measuring the power. Table 1 shows the power measurements taken and the calculated percentage of IR light that was passed through the filter.

	1000 nm setting		
	P_{total} (mW)	P_{850} (mW)	% IR Light
15 cm	118.0	107.4	91.0%
23 cm	52.1	46.8	89.8%
30 cm	27.0	24.2	89.6%
	1064 nm setting		
	P_{total} (mW)	P_{850} (mW)	% IR Light
15 cm	148.0	134.0	90.5%
23 cm	42.2	38.7	91.7%
30 cm	22.2	20.0	90.1%

Table 1. Power measurements of the Torch flashlight for determining percentage of IR light.

Additionally, to verify that the Torch flashlight emits mostly IR light, temperature measurements of the 0.1 wt% SWNT-LCE/silicone bilayer film were also taken using different filters. Figure 11 shows the temperature profile of a 0.1wt% SWNT-

LCE/silicone bilayer film as it is being irradiated for 10 seconds with the Torch at a distance of 23 cm with different filters. The temperature measurements of the film was compared as it was irradiated first with only the Torch, then with IR light (using an 850 nm cut-on filter with the Torch) and visible light (using a 483 nm filter with the Torch). The 850 nm filter allows light with a wavelength range greater than 850 nm to pass through the filter. The 483 nm filter allows light with a wavelength range from 365-650 nm to pass through the filter.

The maximum temperature after 10 seconds of irradiation with just the Torch was 81.4 °C. Using the Torch with an IR filter, the temperature was 74.6 °C. Using the Torch with a visible filter, the temperature was 34.1 °C. Sample temperatures of 0.1 wt% SWNT-LCE/silicone bilayers were measured with a MICRO-EPSILON thermoMETER LS non-contact infrared thermometer. Note that the temperature difference for the IR filter is only 8%. Whereas the difference in temperature for the visible filter is 58%. From these data, it can be seen that most of the light that comes out of the Torch flashlight is IR light since the temperature of the 0.1 wt% SWNT-LCE film was similar when the IR filter was used.

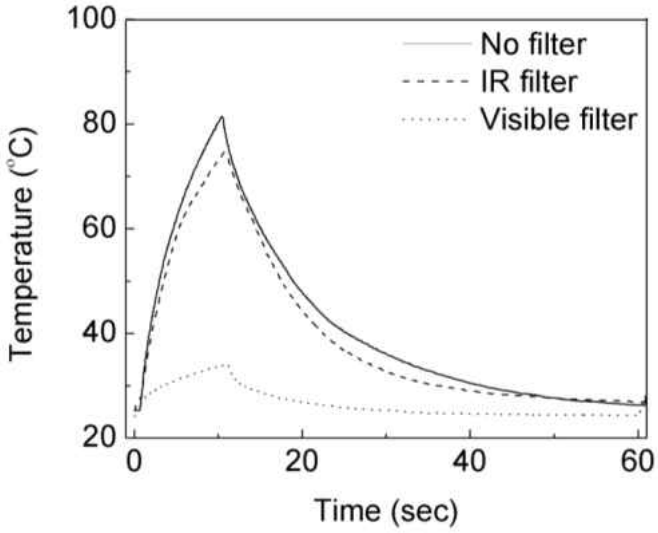

Figure 11. Temperature profile of 0.1 wt% SWNT-LCE/silicone bilayer film with different filters.

F.2. Preparation of the Foldable Structure

A grey scale diagram of the foldable structure is shown in Figure 12. The foldable structure consists of four PC films (L = 5 mm, w = 5 mm, t = 94 μm) and three 0.1 wt% SWNT-LCE/silicone bilayer films (L = 5 mm, w = 5 mm, t_1 = 258 μm , t_2 = 157 μm).

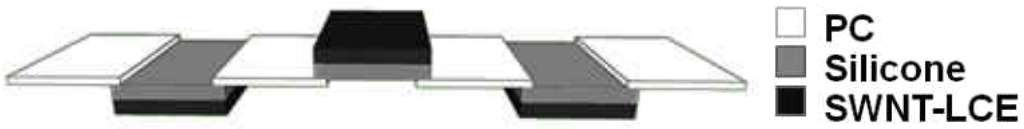

Figure 12. Schematic diagram of the foldable structure.

The assembly of the foldable structure consists of three parts (one "head" and two "arms"). The "head" consists of the central bilayer. The "arms" consist of the two symmetric parts on each side of the center bilayer film. Each arm consists of one bilayer film and two PC films. The arms were assembled and then attached to the head.

To make an arm, a thin layer of silicone adhesive was applied to two opposite edges of the bilayer. The adhesive was applied to the silicone side of the bilayer. Next, the PC films were attached to those edges. The adhesive applied was allowed to dry for 4 h at room temperature. After drying, the arms were oriented with the LCE side down. Silicone adhesive was then applied to one edge of one PC film from each arm, and the central bilayer film was attached. The adhesive was allowed to dry for 4 h at room temperature.

F. 3. Preparation of the Short and Long Grabber

Two grabbers were made: the short grabber and the long grabber. The short and the long grabber were both made with three 0.1 wt% SWNT-LCE/silicone bilayer films and two curved PC films. The dimensions of the three 0.1 wt% SWNT-LCE/silicone bilayer films were similar for both the short and the long grabber. However, the PC films have different dimensions for the grabbers. The short grabber is made with two PC films that are 10 mm by 15 mm long, whereas the long grabber is made with two PC films that are 10 mm by 25 mm long. The purpose of having a longer PC arm will be discussed later in this thesis. Figure 13 shows a diagram of a grabber.

The short grabber (15 mm PC arms) was made with three 0.1 wt% SWNT-LCE/silicone bilayer films (L = 23 mm, w = 2 mm, t_1 = 244 μm , t_2 = 143 μm) and two curved PC films (L = 15 mm, w = 10 mm, t = 111 μm). Three 0.1 wt% SWNT-LCE/silicone bilayer films(spaced apart by 2 mm) versus one large 0.1 wt% SWNT-LCE/silicone bilayer film was done to conserve LCE material. Not only that, but it is difficult to prepare larger 0.1 wt% SWNT-LCE films because they tend to break during the stretching process when the films are being prepared.

To make curved PC films, rubbing in one direction was applied along the length of the PC films on the top side. This rubbing caused the PC films to curve upwards, similar to curling a ribbon with scissors. Three 0.1 wt % SWNT-LCE/silicone bilayer films were placed next to each other and spaced 2 mm apart. Silicone adhesive was applied to the silicone side of the bilayer films. One PC film was first attached to the same side of each end of the three bilayer films. Next, the second PC film was attached to the opposite end of the bilayers. The adhesive was allowed to dry for 4 h at room temperature. Silicone adhesive was then used to attach one end of a 0.66 mm diameter metal wire to the silicone side of the center bilayer film. The metal wire served as the handle of the short grabber. The metal wire is not shown in Figure 13.

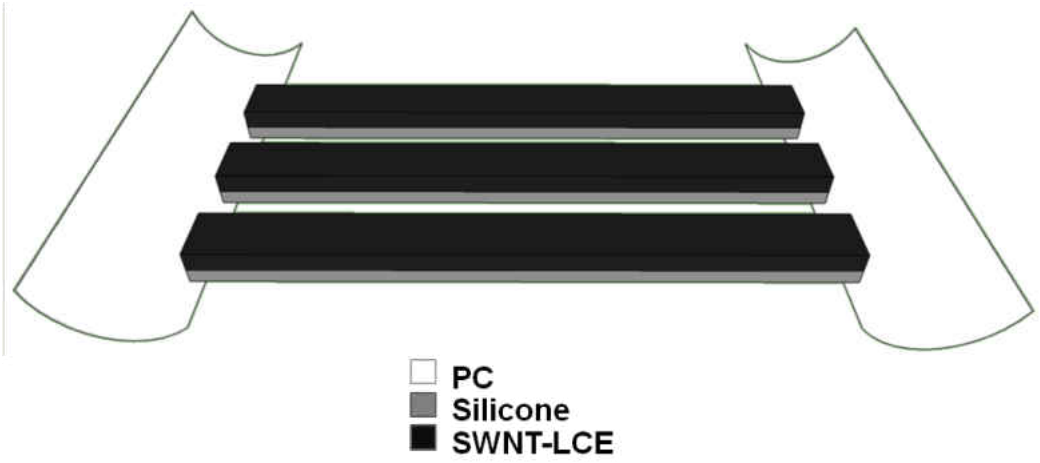

Figure 13. Schematic diagram of the grabber.

The long grabber (25 mm PC arms) was made also made with three 0.1 wt% SWNT-LCE/silicone bilayer films (L = 23 mm, w = 2 mm, t_1 = 244 μm , t_2 = 143 μm) and two curved PC films (L = 25 mm, w = 10 mm, t = 111 μm) and prepared the same way the short grabber was prepared. Two 25 mm additional wires were attached to the center of the PC films along the length, to increase its rigidity. The thin PC films were too flimsy in the water and needed extra reinforcement to hold their shape in water.

F. 4. Preparation of the Crawler

The crawling device (shown in Figure 14) was made using one 0.1 wt% SWNT-LCE film (L = 15 mm, w = 3 mm, t = 243 μm), two silicone films of different lengths, and two differently shaped PC films.

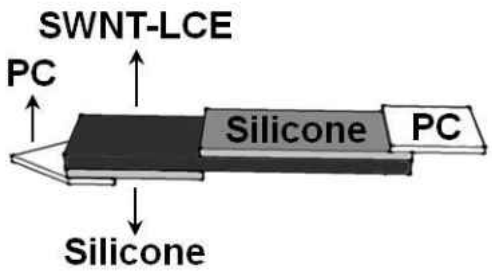

Figure 14. Schematic diagram of the crawler.

To construct the crawler, a silicone adhesive was used to attach the SWNT-LCE film to a 149 μm thick silicone film and allowed to dry for 24 h. A razor was used to cut out the silicone film so its length and width were similar to that of the SWNT-LCE. The opposite side of SWNT-LCE film was then attached to another silicone film and allowed to dry for 24 h.

Once dried, the second silicone film was cut to similar dimensions as the SWNT-LCE film. From one end of the trilayer, 6 mm of silicone film was cut and peeled off the top of the SWNT-LCE film. From the opposite end, 9 mm of silicone film was cut and peeled off the bottom layer of the SWNT-LCE film.

To make the head of the crawler, a pentagonal shaped PC film (with dimensions: 3 mm, 3 mm, 2 mm, 3mm, and 2 mm, t = 94 μm) was attached to the bottom silicone film using a silicone adhesive. A PC film (L = 4 mm, w = 3 mm, t = 108 μm) was attached to the top silicone film.

G. Preparation and Characterizations of 0.2 wt% Dye 1002-LCE/Silicone Bilayer Hinges

To make the 0.2 wt% Dye 1002-LCE/silicone bilayer, a 0.2 wt% Dye 1002-LCE film (L = 10 mm, w = 3 mm, t = 244 μm) was attached to a silicone film (L = 10 mm, w = 3 mm, t = 158 μm). A thin layer of freshly mixed 1:1 Ecoflex 00-30 Part 1A and Part 1B was applied as an adhesive to 0.2 wt% Dye 1002-LCE film. A razor was used to remove the excess liquid. The 0.2 wt% Dye 1002-LCE film was gently placed onto the silicone film. The silicone adhesive was allowed to cure at room temperature for 24 h. Once the silicone adhesive dried, a razor was used to cut the silicone film, matching the silicone length and width to that of the 0.2 wt% Dye 1002-LCE length and width.

For wavelength selectivity experiments, 500 mW of 980 nm and 1342 nm near IR lasers were used with a calibrated power intensity of 2.55 mW/mm^2. Calibration of the IR laser sources was measured using a Newport power meter model 1918-C with an IR detector (918D-IR-OD3).

III. Experimental Data and Discussion

A. 0.1 wt% SWNT-LCE/Silicone Bilayer Hinges

A. 1. Bending of 0.1 wt% SWNT-LCE/Silicone Bilayer Hinges

This section focuses on the bending motion of a 0.1 wt% SWNT-LCE/silicone bilayer structure. This bending was achieved by attaching a reversible contracting and elongating LCE film (active layer) to a flexible silicone film (passive layer). Upon Torch irradiation, heating of the LCE film causes it to contract while the silicone layer remains unchanged. This difference in thermal response allows the bilayer film to bend toward the LCE side. Figure 15 illustrates the bending motion of the bilayer film.

Figure 15. Illustration of 0.1 wt% SWNT LCE/silicone bilayer film when irradiated.

Images of a 0.1 wt% SWNT-LCE/silicone bilayer film is shown in Figure 16, (dimensions: L = 23 mm, w = 3 mm, t_1 = 253 μm, t_2 = 152 μm) as it is being irradiated with the Torch at a distance of 23 cm. After 10 seconds of irradiation, the film reaches maximum bending. As the Torch is turned off and the film cools, it also relaxes to its original state.

Figure 16. Photo images of a 0.1 wt% SWNT-LCE/silicone bilayer film as it responds to IR irradiation.

With this experiment, temperature and curvature measurements were also taken. Figure 17 shows the temperature profile of the bilayer film under 3 cycles of IR irradiation (on for 10 seconds, off for 50 seconds). The maximum average temperature for three cycles was 81.8 +/- 0.6 °C. The average maximum curvature for three cycles was 0.26 +/- 0.01 mm^{-1}.

Curvature calculations were done by drawing a best fitting circle to each film at maximum bending. The equation for curvature is shown in Equation 4, where *R* is the radius of the best fitting circle. To determine the error, curvature was calculated for 3 cycles for each bending experiment.

$$Curvature = 1/R \quad (4)$$

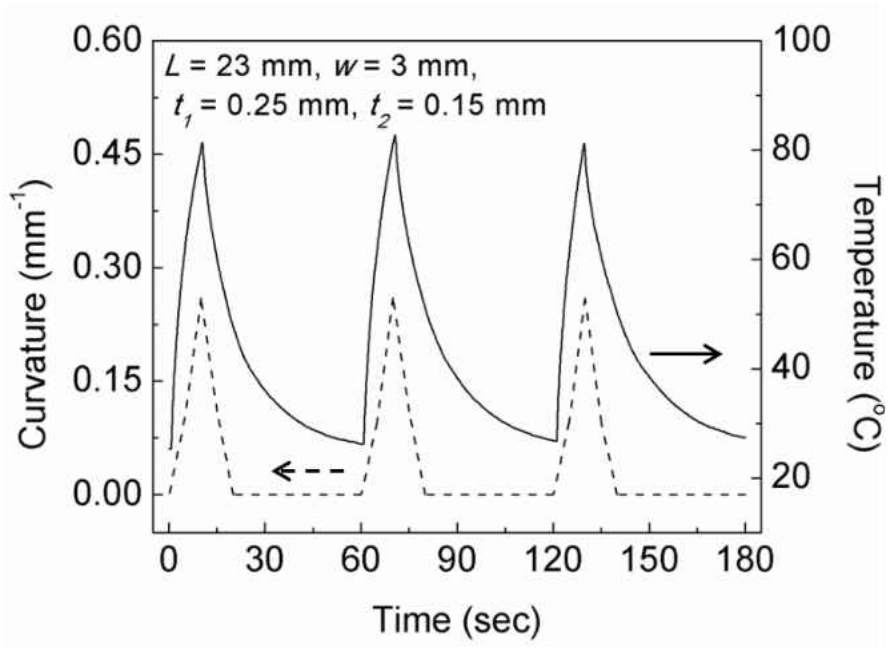

Figure 17. Curvature (dashed line) and temperature measurements (solid line) of a 0.1 wt% SWNT-LCE/silicone bilayer film.

Curvature was also compared for 0.1 wt% SWNT-LCE/silicone bilayer films with varying silicone thicknesses. For this experiment curvature measurements of 14 mm bilayer films (L = 14 mm, w = 3 mm, t_1 = 253 μm, t_2 = 152 μm, 346 μm, or 655 μm) were compared with 23 mm bilayer films (L = 23 mm, w = 3 mm, t_1 = 253 μm, t_2 = 152 μm, 346 μm, or 655 μm). Figure 18 shows the images of the films after 20 seconds of IR irradiation from a distance of 15 cm. From the images, it is observed that as thickness of the silicone film increases, the curvature of the films or the bending of the films decrease.

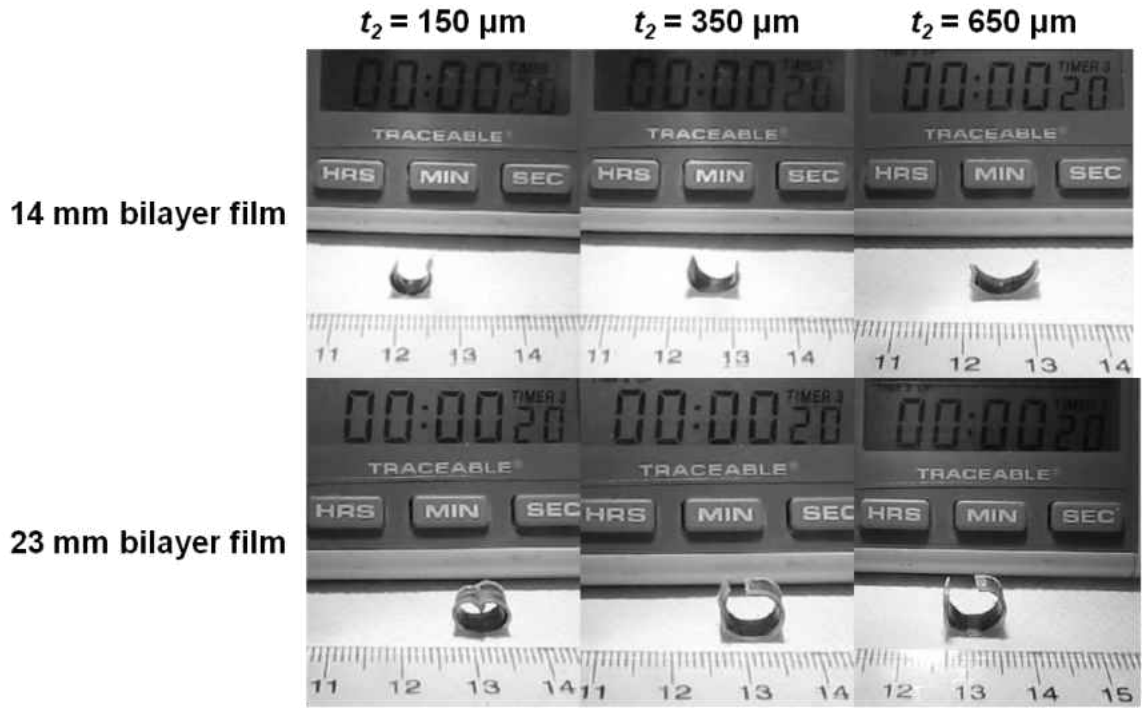

Figure 18. Bending of 14 mm versus 23 mm 0.1 wt% SWNT-LCE/silicone bilayer films with varying silicone film thicknesses (t_2) .

Curvature of the 0.1 wt% SWNT-LCE films were plotted against silicone thickness in Figure 19. Each experiment consisted of three cycles. Turning the IR source on for 20 seconds and off for 40 seconds represented one cycle. The standard deviation was calculated from the average difference in curvature for those three cycles. For most of the plots, the standard deviation of curvature fell within +/- 0.03 mm^{-1}.

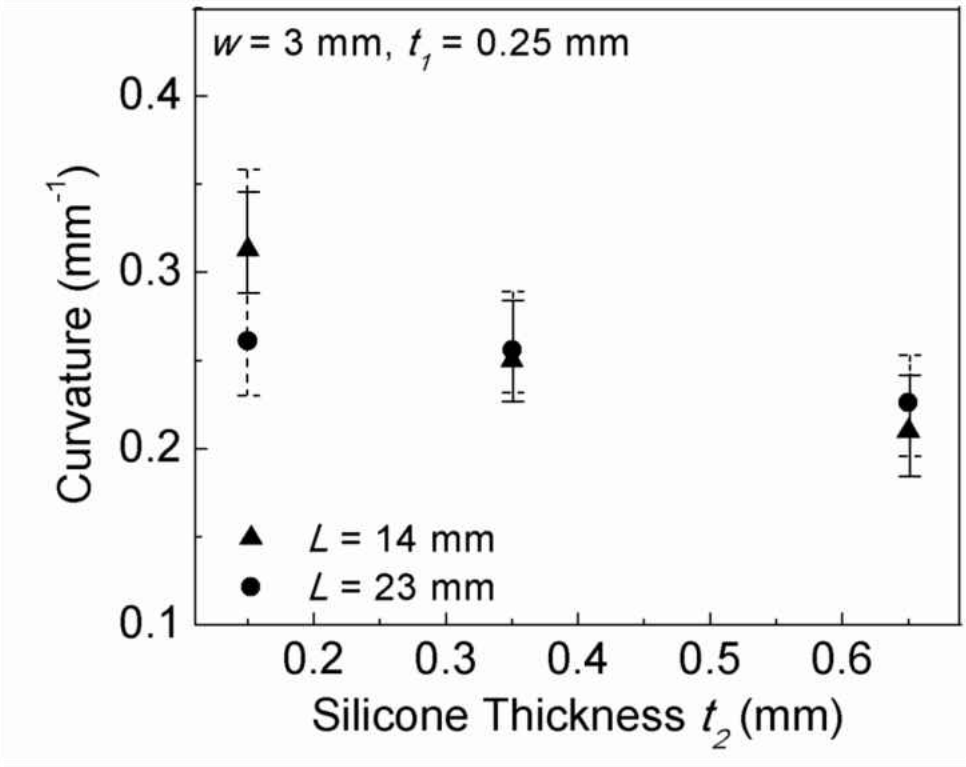

Figure 19. The effect of silicone thickness on curvature of 14 mm and 23 mm bilayer films with error bars.

Note that there is a different standard deviation (+0.1/-0.03 mm^{-1}) for the 23 mm bilayer film when attached to a silicone layer (t_2) that was 150 μm in thickness. The lower limit takes into consideration the average difference among the three cycles. The higher limit takes the side arms into consideration, where there is more bending. This could be due to the fact that the arms of the film of the 23 mm bilayer film are touching when irradiated, causing the arms to curl upon themselves. Another reason is that the arms are slightly closer to the IR source since the light source is directly above and therefore has slightly more bending at the top than at the bottom. And lastly, the middle

of the film is anchored by its own weight at the bottom whereas the weight of the film itself has less force on the side arms. Because of these aspects, it was more difficult to draw a best fitting circle and harder to obtain a more accurate curvature measurement for the 23 mm bilayer film than for the 14 mm bilayer film.

A. 2. Devices made from 0.1 wt% SWNT-LCE/Silicone Bilayer Hinges

There were 3 devices that were made with bilayer hinges: a folding structure, a grabbing structure, and a crawling structure.

A. 2. 1. Foldable Structure

A schematic diagram of the design of the foldable structure is illustrated in Figure 20a. The bilayer films in this structure were arranged in opposite directions to allow for bending in zig-zag form. The purpose of this folding structure was to be able to create a functioning structure that can lift an object up and down as the structure folds and unfolds, similar to a jack.

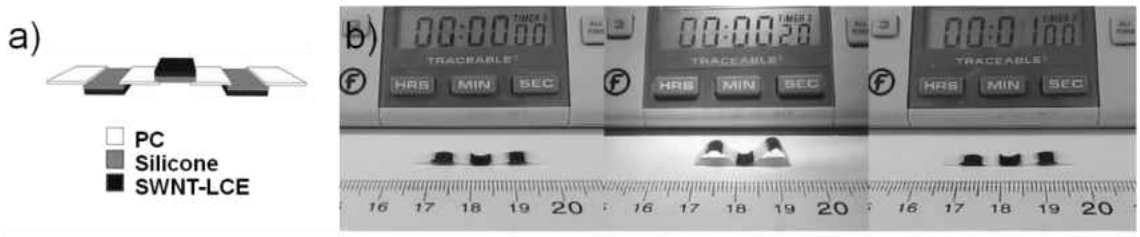

Figure 20. a) Schematic illustration of the foldable structure. **b)** Folding and unfolding of the foldable structure as IR source is turned on and off.

Figure 20b demonstrates the zig-zag form of the folding structure as it is irradiated with the Torch flashlight at a distance of 23 cm. Once the Torch flashlight is turned off, each bilayer film relaxes and the folded structure returns to being flat on the surface again. Although the folding structure can move up and down it was unable to lift anything more than 0.17 g of weight.

A. 2. 2. Grabber

The second device that was made was a grabber. Figure 21 shows the grabber bending upon irradiation. As the Torch flashlight is turned on from a distance of 15 cm, the 0.1 wt% bilayer films begin to bend. This allows the PC films (serving as the claws of the arms) to close within 10 seconds. Turning off the IR source after 10 seconds causes the bilayer films to relax and allows the PC claws to open again.

Figure 21. Closing and opening of the hinge is demonstrated.

Two different grabbers were made: a short grabber (15 mm curved PC claws) and a long grabber (25 mm curved PC claws). Figure 22a and Figure 22b show photo images

of these two different grabbers. The dark line that runs along the center of the PC claws in Figure 22b are the metal wires that reinforce its shape under water.

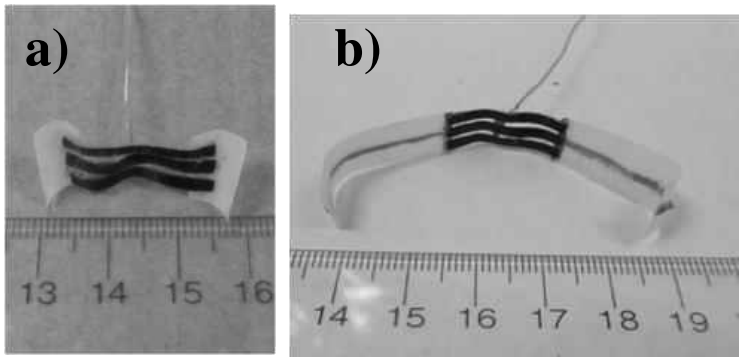

Figure 22. a) Photo image of the short grabber. **b)** Photo image of the long grabber.

The short grabber has the ability to pick up small objects (weighing less than 4 g) in air. Figure 23a and Figure 23b show that the short grabber can pick up 3 g but no more than 4 g. This experiment demonstrates the limitation on weight of the short grabber.

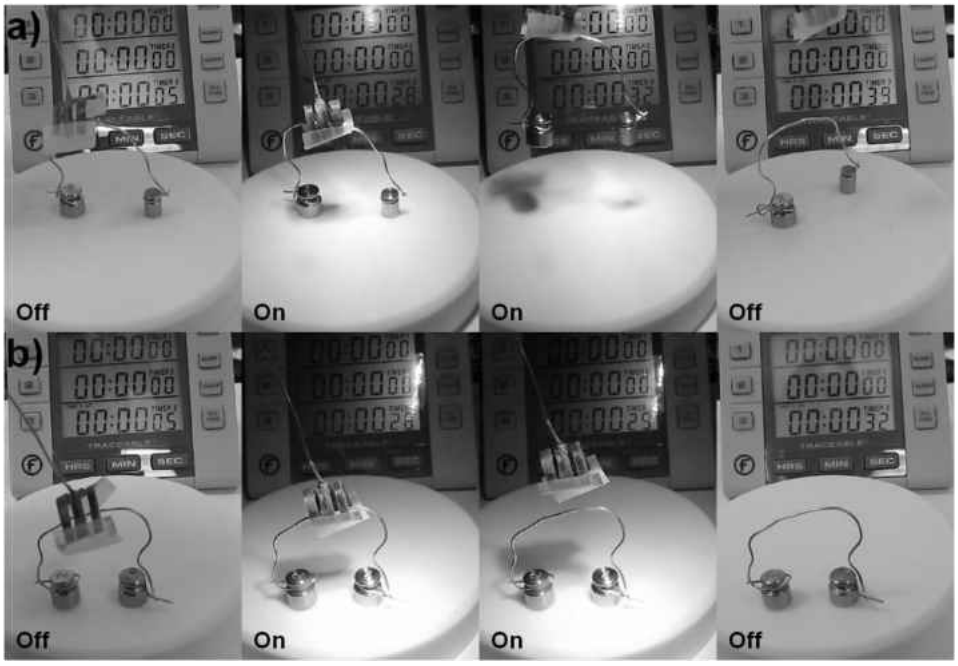

Figure 23. a) Photo images showing the grabber can pick up and object of 3.37 g.

b) Photo images showing the grabber is unable to pick up an object of 4.37 g.

The short grabber can be used to pick up objects of different forms and sizes as shown in Figures 24a and 24b because of the elasticity of the bilayer films. In Figure 24a, a safety pin weighing 0.37 g can be readily picked up and placed on a different object. The light source is turned on at 5 seconds. After 10 seconds of irradiation, the bilayer films reach maximum bending. The PC claws are then wrapped around the safety pin and it is relocated. When the object is in the air (unsupported), irradiation is required to keep the grabber closed. Once the safety pin is placed back onto a surface, the IR source is turned off and the grabber relaxes, its claws open and the safety pin is released.

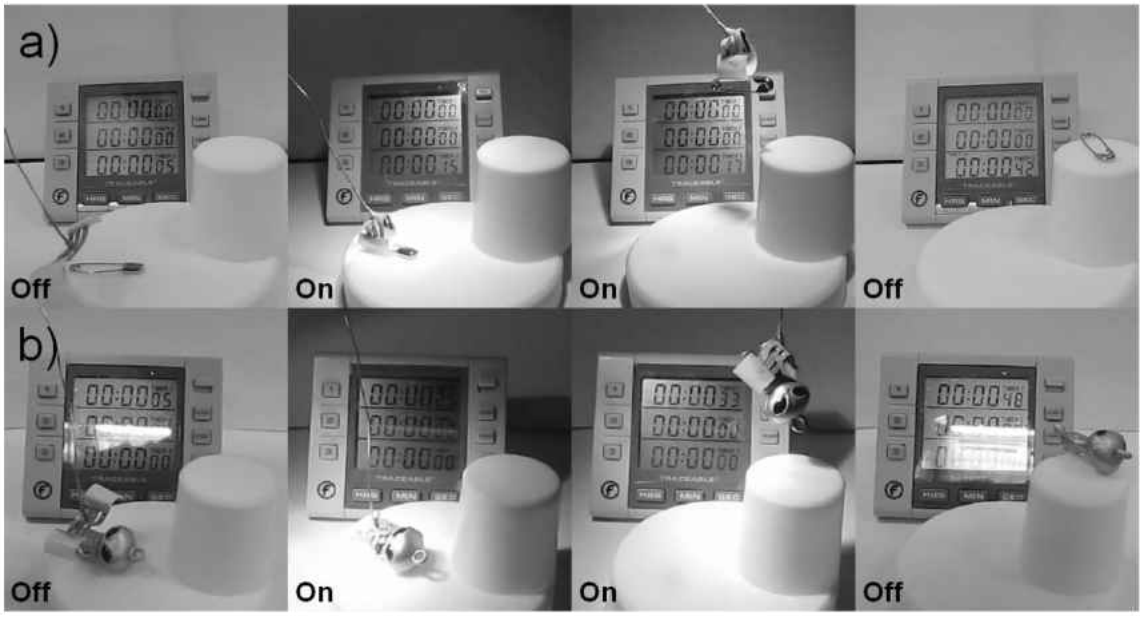

Figure 24. The short grabber lifts **a)** a safety pin of 0.37 g and **b)** a toy alien of 3.97 g.

Figure 24b shows a similar demonstration moving a toy (in this example, and "alien") weighing 3.97 g. The light source is turned on at 5 seconds. Since the weight of the toy is more than that of the safety pin and is very close to the maximum weight that the grabber can handle, it takes quite some effort to lift the toy without putting too much strain on the grabber. After placing the toy on a different surface, the IR source is turned off and the grabber releases the toy.

The ideal grabber has the ability to lift not only objects in air but also from under water. When submerging the short grabber into water, the bilayer films were unable to bend due to its inability to heat up under water. This is probably due to water absorbing much of the IR light. The long grabber was then modified in such a way that only the PC claws are submerged under water. The bilayers needed to remain above the water level in order for them to function properly.

Figure 25 shows the long grabber as it is used for picking up an object under water. The long grabber is first shown in its relaxed state with no irradiation. The long grabber is then placed into the water with the PC claws under the water level but making sure that the 0.1 wt% SWNT-LCE/silicone bilayer films are above the water level. Once the IR source is turned on, the bilayer films begin to bend and the PC claws start to close around the object. After 20 seconds, the 1.21 g object is lifted out of the water and placed on top of a dry surface. The IR source is turned off and the grabber releases the object.

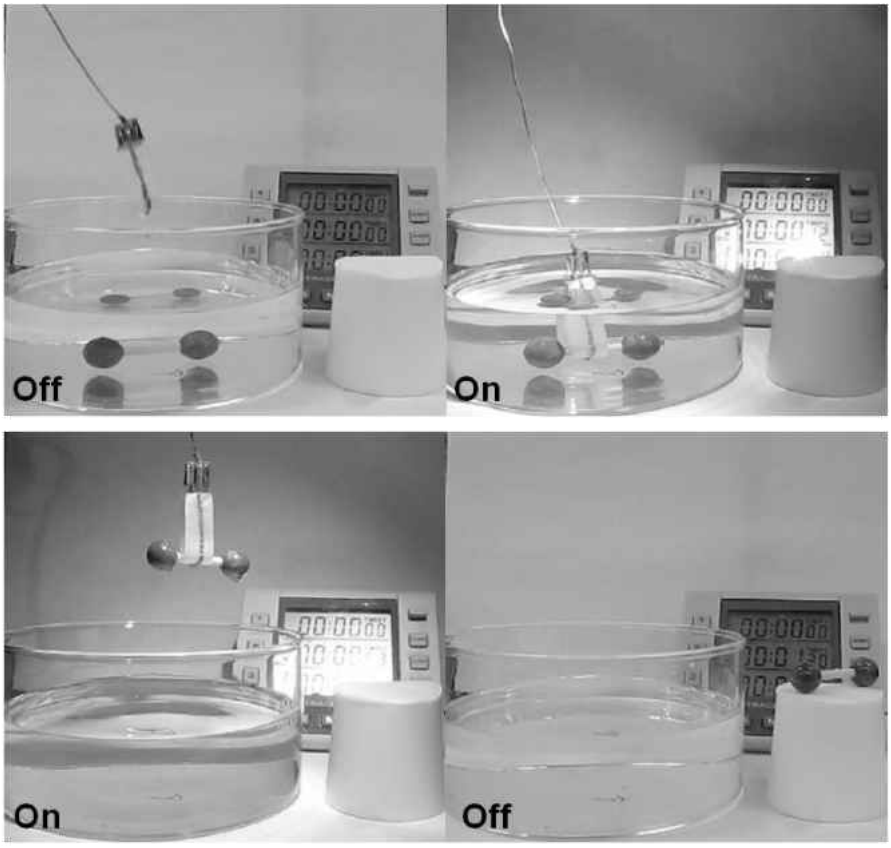

Figure 25. The long grabber lifts an object out of water.

A. 2. 3. Crawler

A crawling device was also constructed using the bilayer bending hinge. A top view photo image of the crawler is shown in Figure 26a. Figure 26b schematically shows the different layers that make up the crawler. A ratchet patterned track was etched onto a wood surface to aid the crawler in sliding upwards at an incline of 50°. Figure 20c shows an exaggerated image of the etch marks on the wood surface. The track on the wood prevents the tail of the crawler from slipping downwards and enables upward crawling of the device.

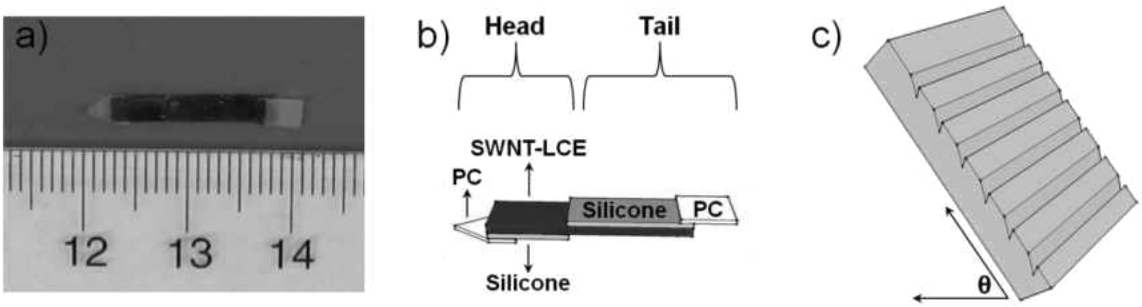

Figure 26. a) Photo image of the top view of the crawler. **b)** Schematic diagram of the crawler. **c)** Schematic drawing of the track on the wood surface to prevent the tail from sliding downwards**.**

Figure 27 shows the first, middle, and last cycles of the crawling device as it moves upwards on the wood surface. The light source is turned on and aimed at the head (see Figure 21b) of the crawler first. This allows the head to bend upwards and anchors the top half of the crawler on to the wood substrate. The light source is then moved to the

mid-tail section of the crawler. This allows for the bottom half of the crawler to bend downwards. As the head is still anchored at the top, the bottom of the crawler moves upwards as it bends. The light source is then removed and the bilayer films of the crawler start to relax. As the crawler unbends, the PC foot of the tail on the crawler slides downwards until it is stopped by one of the etch marks on the wood surface. This makes it possible for the crawling device to slide forward as it unbends. Turning on and off the light source allows the crawler to move upwards on a wood surface at a 50° incline.

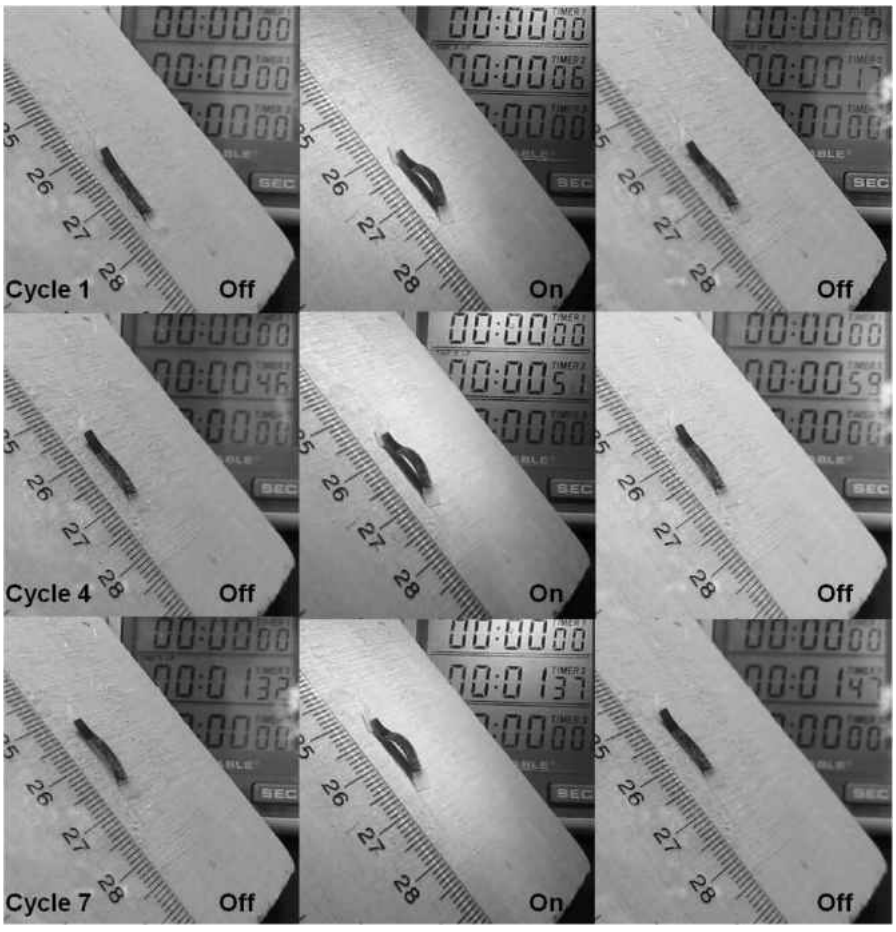

Figure 27. First, middle, and last cycles of the crawler as it moves upward on a wood surface.

B. 0.2 wt% Dye 1002-LCE/Silicone Bilayer Hinges

The second hypothesis to be tested is the wavelength selectivity feature of LCE films. In this section, the filler that was chosen was an organic dye. In chloroform, the maximum absorbance is found at 1007 nm (see Figure 28a, dashed line). When Dye 1002 is mixed into the LCE matrix, the maximum absorption of the 0.2 wt% Dye 1002 LCE film is found at 1034 nm (see Figure 28a, solid line). Note that the baseline absorbance of the 0.2 wt% Dye 1002 LCE film is higher than that of the Dye 1002 solution in chloroform. This is probably due to the solution being more transparent than the film, in example, light scattering occurs within the film.

The IR lasers that were used to test the wavelength selectivity of the 0.2 wt% Dye 1002 LCE film were a 980 nm IR laser and a 1342 nm IR laser. From the absorbance spectrum of the 0.2 wt% Dye 1002 LCE film, the absorbance at 980 nm (1.58 a.u.) is three times higher than that of the absorbance at 1342 nm (0.52 a.u.). With this in mind, the 0.2 wt% Dye 1002 LCE film is expected to heat up more when it is irradiated with the 980 nm laser.

Figure 28b shows the temperature profiles for three on/off cycles of the 0.2 wt% Dye 1002 LCE/silicone bilayer film under the two different laser sources. When the bilayer film is irradiated with 2.55 mW/mm^2 of the 980 nm laser source, the temperature of the 0.2 wt% Dye 1002 LCE layer increases to 68.7 +/- 0.2°C. When the bilayer film is irradiated with 2.55 mW/mm^2 of the 1342 nm laser source, the temperature of the 0.2 wt% Dye 1002 LCE layer heats up to 32.0 +/- 0.2°C. For each of the laser sources, the

error of the reported temperature measurements was calculated by subtracting the maximum temperature at each cycle from the maximum average temperature.

Other errors in temperature measurements that I would like to also discuss are the variance of temperature measurements, possibly due to non-uniform films or fluctuations in the room temperature. Uniform films will have evenly dispersed mixers. When the LCE film is being prepared, it can be difficult to evenly spread the thick melted liquid across the teflon substrate. The thickness of a typical 0.2 wt% Dye 1002 LCE film varies from +/- 12 μm. The softness of the LCE material can also make it difficult to measure thickness.

The temperature of the room and air flow through the room may also affect the temperature of the film. On cooler days, with the room temperature at 19 °C (versus normal room temperature of 23 °C), the temperature of the film can be found to be 4 °C lower. More air flow through the room may also cause the maximum temperature to be lower. With these variables in mind, the error for temperature measurements of 0.2 wt% Dye 1002 LCE films has been found to be +/- 5 °C.

There are a few things that can be controlled better for collecting more accurate temperature measurements. To decrease the variability in temperature, it would be preferable to start measuring the temperature as it increases from a set initial temperature, such as 25 °C. Additionally, more 0.2 wt% Dye 1002 LCE samples should be made for a better comparison. For these experiments, only two films were used. It would also be better to compare film thickness as a function of temperature to determine how much

thickness contributes to temperature variation. Controlling the air flow or minimizing air flow through the room should also allow for a more accurate temperature reading.

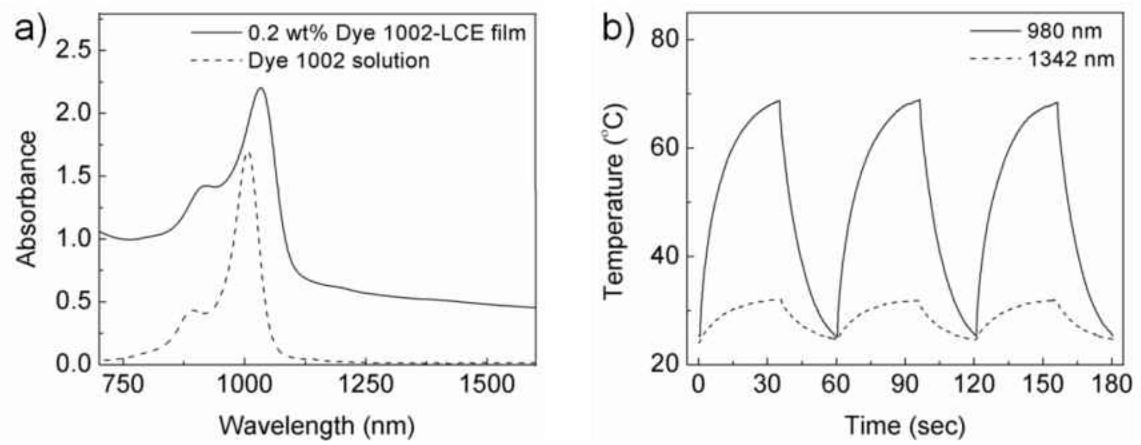

Figure 28. a) UV-Vis-NIR absorbance spectra of Dye 1002 solution in chloroform and 0.2 wt% Dye 1002-LCE film. **b)** Temperature profiles of 0.2 wt% Dye 1002-LCE/silicone elastomer bilayer film under 980 nm and 1342 nm laser irradiation at the same intensity (2.55 mW/mm^2).

Along with the temperature profiles are images obtained when subjecting the 0.2 wt% Dye 1002-LCE/silicone bilayer film to different IR laser sources. Figure 29 shows that upon irradiation of the 980 nm laser at 2.55 mW/mm^2, bending was observed. Whereas under 2.55 mW/mm^2 of 1342 nm laser irradiation, no bending was observed. The DSC results shown in Figure 8 supports these observations. Since the 0.2 wt% Dye 1002-LCE film does not heat up to the T_{NI} (64.4 °C) under the 1342 nm laser, the 0.2 wt% LCE film does not contract. Therefore, the bilayer film does not undergo bending.

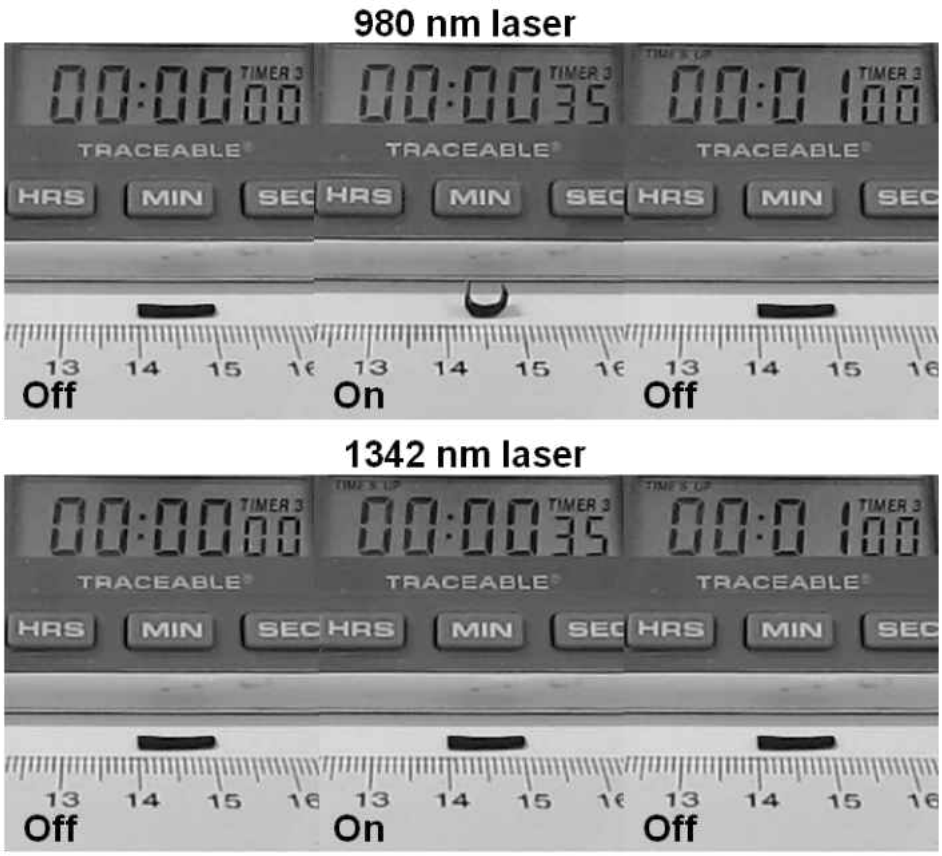

Figure 29. Wavelength selectivity of 0.2 wt% Dye 1002-LCE/silicone elastomer bilayer film as it bends under a 980 nm laser but not a 1342 nm laser source.

I V. Other Concerns

A. 0.1 wt% SWNT-LCE/silicone Bilayer Bending Experiments

There are a few things to discuss in terms of experimental design and possible errors. For the 0.1 wt% SWNT-LCE bending experiments (14 mm and 23 mm 0.1 wt% SWNT-LCE/silicone bilayer with varying silicone film thickness), increasing the time of the experiment should be further explored. The experiment, although irradiated with three cycles, was done only once. One 23 mm 0.1 wt% SWNT-LCE film was used to study the effect of silicone thickness on bending (t_2 = 150 μm, 350 μm, 650 μm). Although this is a good control, it was noted that subjecting LCE films to higher intensities (i.e., heat the film past ~150℃) can damage the film. It has also been noted that some films, after being irradiated repeatedly, started to bend differently , e.g., either by bending less or twisting. Sometimes this issue could be fixed by detaching the LCE film from the silicone film, re-stretching it as much as possible (~290%) and then re-equilibrating the film by thermal annealing (to achieve a final stretching ratio of ~170-180%). To ensure that less bending is not due to hysteresis, the order in which the experiments were done should be altered in such a way that the 0.1 wt% SWNT-LCE/silicone bilayer film with the thickest silicone film (t_2 = 650 μm) is tested first.

Another important factor to consider is the way in which film thickness was measured. Thicknesses of both the LCE films and the silicone films were measured with a micrometer. The measurements were taken by inserting a film within the arms of the micrometer. The arms are then brought together until they touch the sides of the film. For each film, three measurements were taken in three different areas of the film. Both LCE films and silicone films are soft, however silicone films are a lot softer and

sometimes it can be difficult to measure the thickness accurately. It is difficult to tell when the arms actually come in contact with the silicone film or if the arms are applying pressure while it is being closed. In terms of error, it is possible that the actual thicknesses reported could be slightly larger (0-10 μm) than reported.

With these uncertainties, it would be best to do a series of bending experiments with at least two different 0.1 wt% SWNT-LCE films and repeating the experiment for each thickness at least 2-3 times with three on/off cycles. Recording a film's original curvature, how many times it has been irradiated, and its temperature profiles for each irradiation cycle may also help determine how long it takes for hysteresis to occur. This information can also be a helpful for planning and conducting future experiments.

B. 0.2 wt% Dye 1002-LCE/Silicone Bilayer Wavelength Selectivity Experiments

One major concern with the wavelength selectivity experiment is the calibration of the lasers. In terms of wavelength calibration, we were not equipped with an instrument that can confirm the actual output of the 980 nm and the 1342 nm lasers. The instrument that was used to determine the intensity of the laser beams assumes that the lasers are monochromatic. Since this is a very important factor, it is recommended to accurately measure the wavelength of the lasers for further research.

C. Reversible Bending of LCE/silicone Bilayer Films

When exploring types of LCE films with wavelength selectivity capabilities, a major hurdle was encountered: reversibility. While preparing various types of LCE films, reversible bending of a 0.1 wt% SWNT-LCE/silicone bilayer film was easier to obtain than reversible bending of many other types of films. Initial preparation of a 0.1 wt% SWNT-LCE/silicone bilayer film was not reversible. Because the films were not thermally annealed and therefore, not equilibrated properly, the 0.1 wt% SWNT-LCE/silicone bilayer film would bend when it was exposed to IR light but remained bent even after the IR source was turned off. Equilibrating the 0.1 wt% SWNT-LCE film before attaching it to the silicone film allowed the LCE film to be less strained and was an essential step in reversible bending.

When a 0.1 wt% Dye 1002-LCE/silicone bilayer film was initially prepared, it was not reversible even after the 0.1 wt% Dye 1002-LCE film was equilibrated. After a few failed attempts to make reversible films, it was noted that maybe the non-reversible films were may have been cured too long. If a film is fully polymerized, the film consists of many cross-links that do not allow it to elongate once it has contracted. It was hoped that ATR-IR analysis of the curing process could be useful in determining whether a film would be reversible or not. However the ATR-IR measurement did not show a trend between reversible and irreversible films.

The reversible bending of a 0.2 wt% Dye 1002-LCE film was made possible by a trial and error. The parameters that contributed to the degree of polymerization were: curing time, curing intensity, and the amount of filler. From comparing pure LCE films

to reversible 0.1 wt% SWNT-LCE films, it was noted that the pure LCE films were not as soft as the 0.1 wt% SWNT-LCE films. It was also noticed that 0.2 wt% SWNT-LCE films were even softer than 0.1 wt% SWNT-LCE films. The 0.1 wt% SWNT-LCE films have more carbon nanotubes (CNTs) in them than pure LCE films. During the UV curing step, radical polymerization occurs. Since CNTs are radical scavengers, this makes it more difficult for the film to fully polymerize and therefore the 0.1 wt% SWNT-LCE films were softer. By conducting a series of experiments and changing each parameter one at a time, a fully reversible 0.2 wt% Dye 1002-LCE-silicone bilayer film was obtained. For the fully reversible film, increasing the filler from 0.1% to 0.2% and increased the curing time from only 8 min to 9 min.

An interesting study would be to find a method of determining the reversibility of a film. From DSC results of the reversible films, the transition temperature is roughly around 64 ℃. However, irreversible films have transition temperatures ranging between 45 ℃ to 75 ℃. It is possible that the optimal transition temperature for reversible films is around 64 ℃. An LCE film with a high transition temperature (such as 75 ℃) may be too hard whereas one with a low transition temperature (such as 45 ℃) may be too soft.

Other characterization techniques need to be explored to fully understand why some LCE-silicone bilayer films have the capability to bend reversibly. Other ways of characterizing LCE films, such as mechanical tests, may also be helpful to uncover the mystery behind the reversibility of bending. Overall, bending reversibility of these bilayer films is a major issue that should be explored further.

V. Conclusion

Two promising developments for LCE systems were discovered in this thesis. The first development was the successful conversion of IR-induced reversible contraction into IR-induced reversible bending motion, which was then used for fabrication of folding, grabbing, and crawling structures. These functional devices (made from 0.1 wt% SWNT-LCE films) are the first LCE systems to be actuated by IR light instead of UV or visible light. IR actuation of these devices thus expands the list of light sources that can be used for LCE-functioning devices. The fact that three functioning devices were constructed in this thesis also shows the versatility of use for LCE materials.

The second successful development was achieving wavelength selectivity in LCE films with the use of a wavelength specific absorbance filler such as Dye 1002. From the absorption spectrum of 0.2 wt% Dye 1002-LCE film, two laser sources (980 nm and 1342 nm) were used to demonstrate wavelength selectivity for 0.2 wt% Dye 1002-LCE/silicone bilayer films. A reversible bending response was observed under the 980 nm laser source where absorptivity of the 0.2 wt% Dye 1002-LCE film was higher, whereas no bending response was observed under the 1342 nm laser source. Successful wavelength selectivity of 0.2 wt% Dye 1002-LCE films demonstrated how LCEs can be tuned to absorb a specific wavelength range of light.

The new developments discussed in this thesis are significant for LCE systems by adding novel features to it. Only functional devices induced by UV or visible light were reported in previous researchers. In the work described herein, devices made of LCE material also responded to IR light, and not just any IR light but tuned to respond to only a specific range of IR light. The light source used for induction not only was expanded

into the IR region but also controlled to absorb a specific and reasonably narrow wavelength range of light.

VI. References

[1] S. M. Clarke, A. Hotta, A. R. Tajbakhsh and E. M. Terentjev, *Phys. Rev. E: Stat*., *Nonlinear*, *Soft Matter Phys*. **2001**, 64, 061702.

[2] M. Li, P. Keller, J. Yang and P. Albouy, *Adv. Mater.* **2004**, 16, 1922–1925.

[3] G. N. Mol, K. D. Harris, C. W. M. Bastiaansen and D. J. Broer, *Adv. Funct. Mater*. **2005**, 15, 1155–1159.

[4] A. Buguin, M. Li, P. Silberzan, B. Ladoux and P. Keller, *J. Am. Chem. Soc*. **2006**, 128, 1088–1089.

[5] H. Finkelmann, E. Nishikawa, G. G. Pereira and M. Warner, *Phys. Rev. Lett*. **2001**, 87, 015501.

[6] M. Li, P. Keller, B. Li, X. Wang and M. Brunet, *Adv. Mater*. **2003**, 15, 569–572.

[7] T. Ikeda, M. Nakano, Y. Yu, O. Tsutsumi and A. Kanazawa, *Adv. Mater*. **2003**, 15, 201–205.

[8] Y. Yu, M. Nakano and T. Ikeda, *Nature* **2003**, 425, 145.

[9] M. Camacho-Lopez, H. Finkelmann, P. Palffy-Muhoray and M. Shelley, *Nat. Mater*. **2004**, 3, 307–310.

[10] Y. Yu, M. Nakano, A. Shishido, T. Shiono and T. Ikeda, *Chem. Mater.* **2004**, 16, 1637–1643.

[11] K. D. Harris, R. Cuypers, P. Scheibe, C. L. van Oosten, C. W. M. Bastiaansen, J. Lub and D. J. Broer, *J. Mater. Chem*. **2005**, 15, 5043.

[12] M. Kondo, Y. Yu and T. Ikeda, *Angew. Chem., Int. Ed*. **2006**, 45, 1378–1382.

[13] T. Ikeda, J. Mamiya and Y. Yu, Angew. *Chem., Int. Ed*. **2007**, 46, 506–528.

[14] Y. Yu, T. Maeda, J. Mamiya and T. Ikeda, *Angew. Chem., Int. Ed*, **2007**, 46, 881–883.

[15] J. Mamiya, A. Yoshitake, M. Kondo, Y. Yu and T. Ikeda, *J. Mater. Chem*. **2008**, 18, 63–65.

[16] K. D. Harris, C. W. M. Bastiaansen, J. Lub and D. J. Broer, *Nano Lett*. **2005**, 5, 1857–1860.

[17] K. Urayama, S. Honda and T. Takigawa, *Macromolecules*, **2006**, 39, 1943–1949.

[18] D. Shenoy, D. L. Thomsen, III, A. Srinivasan, P. Keller, B. Ratna, *Sens. Actuators A* **2002**, 96, 184.

[19] L. Yang, K. Setyowati, A. Li, S. Gong, J. Chen, *Adv. Mater*. **2008,** 20, 2271-2275.

[20] M. Yamada, M. Kondo, J. Mamiya, M. Kinoshita, C. J. Barrett, and T. Ikeda, *Angew. Chem. Int. Ed*. **2008**, 47, 4986-4988.

[21] M. Camacho-Lopez, H. Finkelmann, P. Palffy-Muhoray and M. Shelley, *Nature. Mater*. **2004**, 3, 307-310.

[22] K. E. Laflin, C. J. Morris, T. Muqeem, and D. H. Gracias, *Appl. Phys. Lett*. **2012**, 102, 131901.

[23] Y. Liu, J. K. Boyles, J. Genzer, M. D. Dickey, *Soft Matter* **2011**, 8, 1764-1769.

[24] R. F. Shepherd, F. Ilievski, W. Choi, S. A. Morin, A. A. Stokes, A. D. Mazzeo, X, Chen, M. Wang, G. M. Whitesides, *PNAS* **2011**, 108, 20400-20403.

[25] F. Ilievski, A. D. Mazzeo, R. F. Shepherd, X. Chen, and G. M. Whitesides, *Angew. Chem. Int. Ed.* **2011**, 50, 1890 –1895.

[26] D. L. Thomsen III, P. Keller, J. Naciri, R. Pink,H. Jeon, D. Shenoy, and B. R. Ratna, *Macromolecules* **2001**, 34, 5868-5875.

[27] J. Chen, H. Lui, W. A. Weimer, M. d. Halls, D. H. Waldeck, G. C. Walker, *J. Am. Chem. Soc.* **2002**, 124, 9034.

VII. Appendix

Online Videos:

1. Bending of 0.1 wt% SWNT-LCE/silicone bilayer film with torch at 23cm distance: https://www.youtube.com/watch?v=0lLbd43iW7g

2. Bending of the foldable structure: https://www.youtube.com/watch?v=3gQpsLhRqPU

3. Short grabber picking up a safety pin: https://www.youtube.com/watch?v=D2GPEzv2yWo

4. Short grabber picking up a toy alien: https://www.youtube.com/watch?v=9c2FxQX3sFc

5. Long grabber picking up an object from water: https://www.youtube.com/watch?v=wPfxdzFmA8Y

6. Crawler on wood surface at 50° incline: https://www.youtube.com/watch?v=d6kWUhgZUNA